Cancer Biol Med 2025. doi: 10.20892/j.issn.2095-3941.2024.0241

ORIGINAL ARTICLE

Chidamide suppresses macrophage-mediated immune evasion and tumor progression in small cell lung cancer by targeting the STAT4/CCL2 signaling pathway

Wenting Liu[1,2*], Ting Mei[1*], Yantao Jiang[1], Jingya Wang[1], Mengjie Li[1], Liuchun Wang[1], Zhaoting Meng[1], Tingting Qin[1], Dingzhi Huang[1]

[1]Department of Thoracic Oncology, Tianjin Lung Cancer Center, Key Laboratory of Cancer Prevention and Therapy, Tianjin's Clinical Research Center for Cancer, Tianjin Medical University Cancer Institute and Hospital, National Clinical Research Center for Cancer, Tianjin Cancer Institute and Hospital, Tianjin Medical University, Tianjin 300060, China; [2]Department of Respiratory Medicine, Beijing Friendship Hospital, Capital Medical University, Beijing 100050, China

ABSTRACT

Objective: This study aimed at exploring the effects of the epigenetic regulator, chidamide, on reprogramming the immunosuppressive tumor microenvironment in small cell lung cancer (SCLC), particularly the roles in macrophage polarization and angiogenesis. The therapeutic efficacy of combining chidamide with the anti-angiogenic agent, anlotinib, for refractory SCLC was also evaluated.

Methods: RNA sequencing and functional validation were performed to assess chidamide's effects on macrophages. Signal transducer and activator of transcription 4 (STAT4)-mediated transcriptional activation of CCL2 was confirmed with ChIP-qPCR. The synergistic efficacy of chidamide in combination with anlotinib was tested in preclinical models.

Results: Chidamide enhanced macrophage infiltration and induced macrophage polarization toward the anti-tumor M1 phenotype. Mechanistically, chidamide upregulated CCL2 *via* STAT4 transcriptional activation, thereby reshaping the tumor immune microenvironment (TIME). Combining chidamide with anlotinib synergistically suppressed tumor growth and remodeled the immunosuppressive TME in SCLC *in vivo*.

Conclusions: Chidamide reshaped the SCLC TIME by activating STAT4/CCL2, thus driving M1 macrophage polarization and enhancing anti-tumor immunity. Our findings highlight coordinated TIME-targeted therapy as a translatable strategy to overcome therapeutic resistance in SCLC and provide a rationale for clinical trials examining epigenetic and anti-angiogenic therapeutics combinations.

KEYWORDS SCLC; chidamide; CCL2; macrophage; tumor immune microenvironment; STAT4

Introduction

As the most aggressive subtype of lung cancer, small cell lung cancer (SCLC) is known for its rapid proliferation and early, widespread metastasis. Most patients with SCLC are diagnosed in advanced stages with a 5-year survival rate < 7%[1]. Patients with SCLC initially respond well to chemotherapy in most cases and often experience significant symptom relief. However, the SCLC high recurrence rate results in an overall poor prognosis. Tobacco exposure, a major etiologic factor in SCLC development, is strongly associated with the high tumor mutation burden[2]. Although a higher tumor mutation burden is generally associated with better immunotherapy responses[3], patients with extensive-stage SCLC have limited survival benefits from chemoimmunotherapy in contrast to patients with non-small cell lung cancer and melanoma[4]. This difference in response to immunotherapy might be primarily attributed to the profoundly immunosuppressive SCLC tumor microenvironment[5,6], which is characterized by diminished cytotoxic immune cell infiltration[7], low PD-L1 expression on tumor cells[8], and impaired antigen presentation[9]. These

*These authors contributed equally to this work.
Correspondence to: Tingting Qin and Dingzhi Huang
E-mail: qintingting@tjmuch.com and huangdingzhi@tjmuch.com
ORCID ID: https://orcid.org/0000-0002-1975-9696 and https://orcid.org/0000-0002-2798-9459
Received May 5, 2025; accepted August 5, 2025;
published online October 23, 2025.
Available at www.cancerbiomed.org

pathophysiologic features collectively undermine the efficacy of current immunotherapeutic approaches. Therefore, developing innovative therapeutic strategies that synergistically inhibit tumor progression and reprogram the immunosuppressive microenvironment in SCLC is a critical unmet need.

According to emerging evidence, epigenetic dysregulation, which is mediated through DNA hypermethylation and histone modification anomalies, is a critical oncogenic driver in SCLC[10,11]. Clinical evidence has confirmed that epigenetic reprogramming critically governs metastatic dissemination, chemoresistance development, and TIME remodeling in SCLC[12-14]. Targeting this dysregulated epigenetic landscape with selective inhibitors has been shown to have therapeutic potential by restoring immunogenic tumor recognition[15] and reinvigorating anti-tumor immunity *via* immune cell functional reprogramming[16,17]. Epigenetic therapeutics might therefore be strategically used as modifiers to normalize the SCLC TIME.

Histone deacetylase (HDAC) dysregulation has prognostic value across multiple malignancies, several HDACs have emerged as potential targets for drug therapy in cancer. Although clinically approved pan-HDAC inhibitors are limited primarily to hematologic neoplasms[18,19], emerging clinical data indicate the therapeutic superiority of subtype-selective HDAC inhibition[20,21]. Chidamide, a first-in-class HDAC1/2/3/10-selective inhibitor, has received regulatory approval for relapsed refractory peripheral T-cell lymphoma and endocrine therapy-resistant metastatic breast cancer in China[22,23] and has demonstrated greater therapeutic precision than conventional pan-HDAC inhibitors[24].

Despite limited preclinical evidence supporting HDAC inhibitor treatment in SCLC, our findings revealed that chidamide exerted dual antitumor effects through direct proliferation suppression and immunomodulatory reprogramming. Mechanistically, chidamide facilitated STAT4-mediated transcriptional activation of CCL2, thereby driving recruitment and M1 polarization of tumor-associated macrophages and establishing an immunostimulatory niche that counteracted SCLC immune evasion. Notably, combination treatment with chidamide and the multi-target tyrosine kinase inhibitor, anlotinib, demonstrated synergistic antitumor efficacy in preclinical SCLC models. Our findings suggested a novel therapeutic paradigm for refractory SCLC through concurrent epigenetic modulation and angiogenic pathway inhibition.

Materials and methods

Cell lines and cell culture

Human SCLC cell lines (SHP77, NCI-H889, NCI-H446, and DMS53), the human mononuclear cell line, THP1, and the murine macrophage cell line, RAW264.7, were obtained from the American Type Culture Collection (ATCC) (Manassas, VA, USA). The mouse SCLC cell line (non-SMC) was a generous gift from Professor Hongbin Ji (Center for Excellence in Molecular Cell Science of the Chinese Academy of Sciences, Shanghai, China) [25]. SHP77, H889, H446, DMS53, and THP-1 cells were grown in RPMI-1640 medium (Gibco, Grand Island, NY, USA) with 10% fetal bovine serum (Gibco, Grand Island, NY, USA). Non-SMC and RAW264.7 cells were cultured in DMEM (Gibco) containing 10% fetal bovine serum. All cells were authenticated with short tandem repeat (STR) profiling and were cultured at 37°C in 5% CO_2.

RNA sequencing

Total RNA was isolated from 0.5 μM chidamide-treated or untreated SCLC cells with TRIzol reagent (15596026; Invitrogen, Waltham, MA, USA), and mRNA was purified with poly-T oligonucleotide magnetic beads. RNA was randomly fragmented with divalent cations. The RNA fragments were subsequently reverse-transcribed to complementary DNA (cDNA), end-repaired, A-tailed at the 3′ end, and adaptor-ligated. The quality and quantity of each cDNA library were tested with a Bioanalyzer 2,100 system (Agilent, Santa Clara, CA, USA). The cDNA libraries were sequenced on the BGISEQ-G400 platform (Wuhan, China) according to commercial protocols. Three groups of RNA samples were extracted from each cell line for sequencing.

Cell apoptosis assays

SCLC cells (SHP77 and non-SMC) that were treated with chidamide or untreated were collected and incubated with Membrane Protein V and 7-AAD (BD Biosciences, San Jose, CA, USA) for 15 min. Apoptotic cells were detected with flow cytometry. Positive staining for Annexin V (PE) (BD Biosciences, San Jose, CA, USA) and negative staining for 7-AAD indicated apoptotic cells, whereas positive staining for

both Annexin V (PE) and 7-AAD indicated late apoptosis. The proportion of total apoptotic cells was calculated as the sum of these two cell populations.

CCK-8 assays

Cells treated with various concentrations of chidamide were seeded in 96-well plates at a density of 3,000 cells per well (0.1 μM, 0.3 μM, 1 μM, 3 μM, 10 μM, and 30 μM) to assess the proliferative ability of cells. CCK-8 reagent (Zeta life, Menlo Park, CA, USA) was mixed with the cells 24, 48, or 72 h after seeding and were incubated at 37°C for 2 h. Absorbance values were measured at 450 nm with a fully automatic microplate reader (Genetech, Shanghai, China).

Western blotting (WB)

SCLC cells were washed with PBS after treatment with chidamide. Cocktail lysis buffer (Roche, Basel, Switzerland) was added to the cell pellet after digestion and centrifugation. The mixture was subjected to ice-cold lysis for 30 min, then centrifuged at 12,000 × *g* for 15 min at 4°C. After collection of the supernatant, the protein concentration was measured with a BCA protein quantification kit (Solarbio, Beijing, China) and equal amounts of protein were separated with 10%–12% SDS-PAGE gel electrophoresis. The proteins were subsequently transferred to PVDF membranes (Millipore, Billerica, MA, USA). After blocking for 15 min at room temperature with protein-free blocking buffer, the membranes were incubated overnight at 4°C with primary antibodies and subjected to three washes with TBST (Solarbio, Beijing, China) and a 1 h incubation with secondary antibodies at room temperature. The following primary antibodies were used: GAPDH (#2118, 1:1000; CST, Danvers, MA, USA); BCL-2 (#3498S, 1:1000; CST); Bax (#2772S, 1:1000; CST); Bim (#2933S, 1:1000; CST); CCL2 (#26161-1-AP, 1:1000; Proteintech, Wuhan, China); H3K27ac (#8173S, 1:1000; CST); HDAC1 (#34589, 1:1000; CST); HDAC2 (#57156,1:1000; CST); HDAC3 (#85057, 1:1000; CST); HDAC10 (ab108934, 1:000; Abcam, Cambridge, MA, USA) and STAT4 (#2653S, 1:1000; CST). Finally, enhanced chemiluminescence reagent (Millipore) was used to detect protein bands on the membrane and the results were captured with a chemiluminescence imager (GelView 6000Plus; Biolight Biotechnology, Guangzhou, China). ImageJ software was used to determine the grayscale density of the protein bands.

Quantitative real time PCR(qPCR)

Total RNA from SCLC cells was extracted with TRIzol Reagent (15596026; Invitrogen) and reverse-transcribed to cDNA with 5× PrimeScript RT Master Mix (RR036A; TAKARA, Tokyo, Japan) with 1 μg of total RNA. qPCR was performed to analyze RNA expression with SYBR Green Master Mix (11184ES03; YEASEN, Shanghai, China) and all reactions were performed in triplicate. The specific primer sequences are provided in **Table S1**.

Immunohistochemistry (IHC) and HE staining

IHC was performed as previously described[26]. Primary antibodies to Ki-67 (#34330, 1:800; CST), CD86 (#19589, 1:100; CST), CD163 (b182422, 1:500; Abcam, Cambridge, MA, USA), CD31 (ab28364, 1:50; Abcam), and CCL2 (1:100; Proteintech) were used. HE staining was performed using a standard protocol. Following dewaxing, the sections were incubated with hematoxylin, then counterstained with eosin.

Enzyme-linked immunosorbent assays (ELISA)

CCL2 chemokine levels in the supernatants of SHP77 and non-SMC cells before and after treatment with chidamide were detected using an ELISA kit (Proteintech) according to the manufacturer's instructions. The absorbance at 450 nm wavelength was measured with a fully automatic microplate reader (BioTek, Winooski, Vermont, USA).

siRNA transfection

Cells were transiently transfected with STAT4 siRNA (Gene Pharma, Shanghai, China) with Lipofectamine 3,000 (Invitrogen) and Opti-MEM (Gibco), according to the manufacturer's instructions. The siRNA target sequences are shown in **Table S2**.

Macrophage polarization

THP-1 cells were induced to polarize into M0 macrophages by incubation in 1 mg/mL of PMA (MedChemExpress, Monmouth

Junction, NJ, USA) for 48 h. Lipopolysaccharide (100 ng/mL; MedChemExpress) and IFN-γ (20 ng/mL; PeproTech, Rocky Hill, NJ, USA) was added to M0 macrophages to obtain M1-polarized macrophages, which were cultured for an additional 48 h. M0 macrophages were cultured with IL-4 (20 ng/mL; PeproTech) and IL-13 (20 ng/mL; PeproTech) for 48 h to generate M2-polarized macrophages. RAW264.7 cells were induced to polarize into M1 macrophages by culturing with IFN-γ (2.5 ng/mL) and lipopolysaccharide (200 ng/mL) for 48 h. RAW264.7 cells were cultured with IL-4 (20 ng/mL) and IL-13 (20 ng/mL) for 48 h to induce polarization into M2 macrophages.

Flow cytometry

Flow cytometry was performed to analyze the influence of chidamide on macrophage polarization in the SCLC TME. Macrophage subpopulations and percentages were assessed with the following antibodies: anti-CD11b (101216; BioLegend, San Diego, CA, USA); anti-F4/80 (123127; BioLegend); anti-CD86 (human-374206 and mouse-105008; BioLegend); and anti-CD163 (human-326510 and mouse-155306; BioLegend). SHP-77 and non-SMC cells treated with chidamide were collected, incubated with the flow cytometry antibodies at 4°C in the dark for 30 min, washed, and resuspended in 200 μL of PBS buffer. The antibody signals were detected using a FACS Calibur flow cytometer (BD Bioscience, San Jose, CA, USA) and data were analyzed using FlowJo v10 software (BioLegend, San Diego, CA, USA).

Co-culture

SCLC cells (SHP77 and non-SMC) were co-cultured with macrophages (THP-1 and RAW264.7). THP-1 or RAW264.7 cells in various states (M0, M1, M2) were seeded in the lower chamber, whereas the upper chamber contained SHP77 or non-SMC cells. The SCLC cells-to-macrophages ratio was adjusted to 5:1. Chidamide or a combination of chidamide and CCL2 neutralizing antibodies were added to the upper chamber after the co-cultured cells in the incubator had reached stability. The macrophages in the lower chamber were collected after incubation in the cell culture chamber for 48 h for subsequent experiments.

Animal experiments

Male BALB/c-nude mice (6-week-old) were purchased from GemPharmatech (Jiangsu, China) and maintained in a pathogen-free environment in the Animal Department of Tianjin Medical University Cancer Institute. This animal study was approved by the Animal Experiment Ethics Committee of Tianjin Medical University Cancer Institute and Hospital [AE-2022004] (Tianjin, China). Non-SMC cells were resuspended in sterile PBS to a density of 5×10^7 cells/mL, then subcutaneously injected into the right dorsum of mice. The mice were randomly divided into a control group (PBS, oral gavage), chidamide group (25 mg/kg, oral gavage, once daily), anlotinib group (2.5 mg/kg, oral gavage, once daily), and combination treatment group (chidamide+anlotinib) when the tumors reached approximately 50–100 mm^3. The tumor volumes and weights of the mice were recorded by a blinded researcher every other day. The first animal experiment included four mice per group (chidamide vs. control). The second animal experiment included six mice per group (chidamide plus anlotinib vs. chidamide vs. anlotinib vs. control). Tumor volume was calculated according to the following formula: $(A \times B^2)/2$, where A and B represent the long and short diameters of the tumor, respectively. The mice were euthanized (cervical dislocation) after 2 weeks of continuous treatment and the tumors were removed and weighed.

Chromatin immunoprecipitation (ChIP)

ChIP assays were conducted with a SimpleChIP Plus Enzymatic Chromatin IP Kit (#9005; CST) according to the manufacturer's instructions. Briefly, approximately 1×10^7 SCLC cells with or without chidamide treatment were fixed in 1% formaldehyde for 10 min at room temperature, then quenched with 0.125 M glycine for 5 min. The cross-linked chromatin was sonicated to generate 100–900 bp DNA fragments for subsequent immunoprecipitation. The protein/DNA complexes were eluted and analyzed with qPCR and the ChIP-qPCR primers listed in **Table S3**.

Statistical analysis

All data were analyzed and visualized in GraphPad Prism 9.0 software (Dotmatics, La Jolla, CA, USA) with Student's *t*-test and one-way ANOVA. The normality and homogeneity of variance were tested before the analysis. Kaplan-Meier analysis was used for survival analysis and the variations in

survival probabilities were evaluated with the log-rank test. The Pearson's rank test was used for correlation analysis between CCL2 expression and other markers. All presented data came from at least three distinct repeated experiments and are expressed as the mean ± SEM. $P < 0.05$ was considered to indicate statistical significance.

Results

Chidamide exhibits anticancer effects in SCLC

RNA-seq data from 81 postoperative patients with SCLC were first analyzed to gain initial insights into HDAC expression[27]. Heat map indicated relatively higher levels of HDAC1, HDAC2, HDAC3, and class II HDAC6 expression compared to other HDACs in patients with SCLC (**Figure 1A**). Chidamide is a subtype selective HDAC inhibitor that predominantly targets class I HDAC1, HDAC2, and HDAC3 and class IIb HDAC10. The differences in expression of the four HDACs between normal and cancer tissues in GSE149507 were subsequently examined[28]. The results indicated significantly higher HDAC1 and HDAC2 expression in SCLC than in cancer adjacent tissues, whereas the changes in HDAC3 and HDAC10 expression were not pronounced (**Figure 1B**). Expression of the four above-mentioned HDACs in SHP77 and non-SMC cells with or without chidamide treatment was determined next. qPCR and WB analyses revealed that HDAC expression decreased to different degrees after chidamide treatment (**Figure 1C, D**).

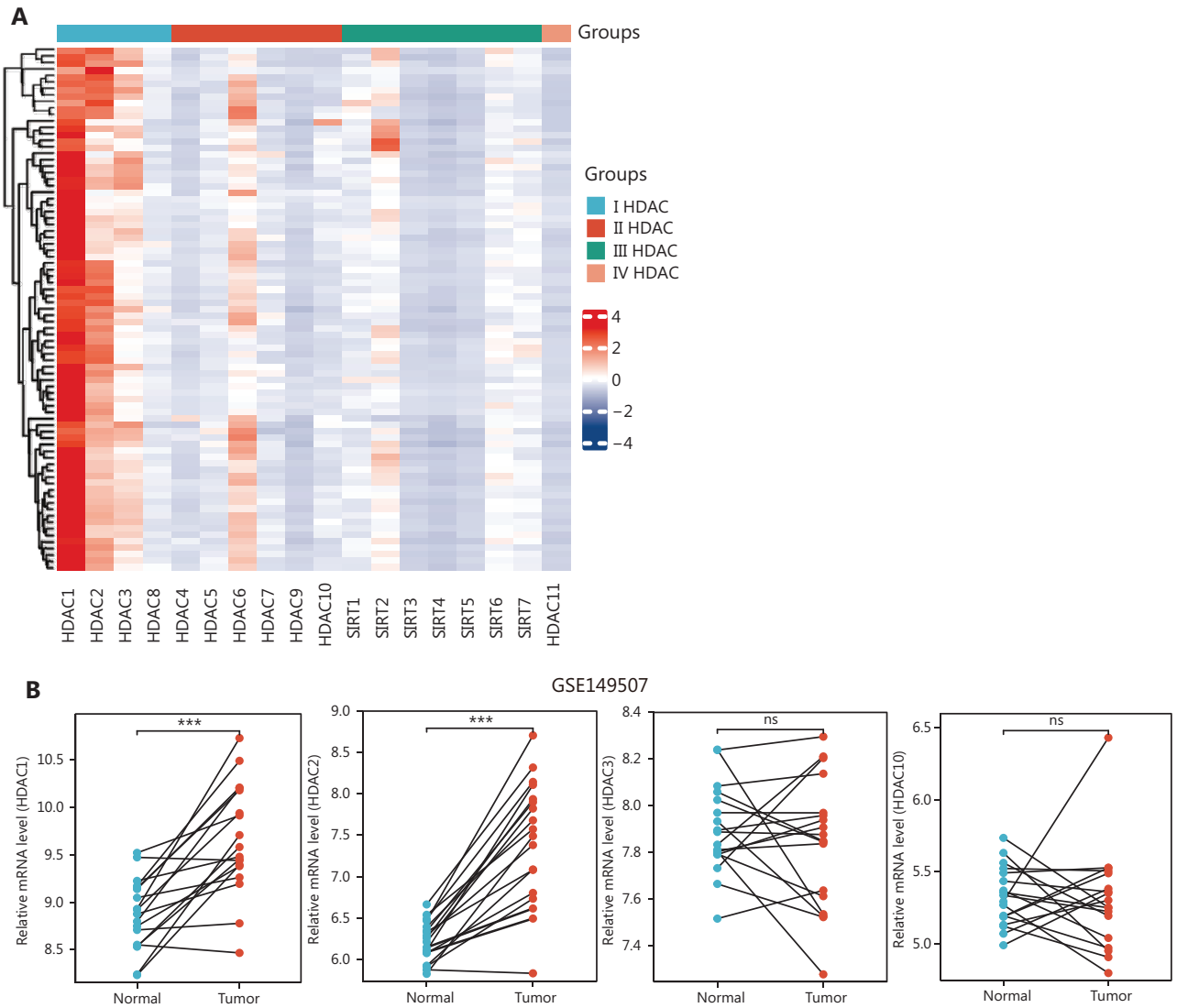

Figure 1 Continued

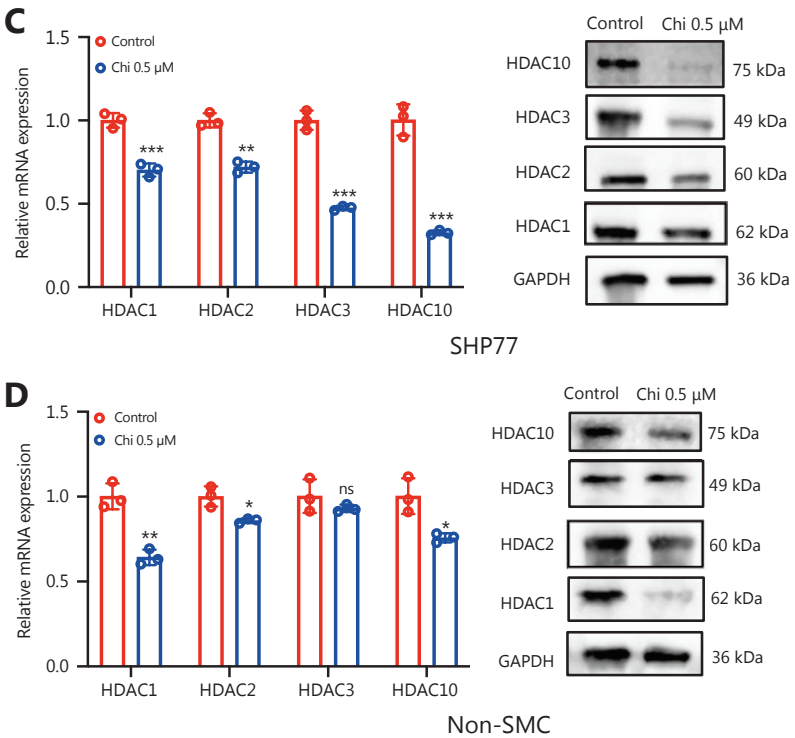

Figure 1 Effects of chidamide on HDAC expression in SCLC. (A) mRNA expression of 18 HDAC types in 81 patients with SCLC. (B) Expression of four chidamide targets in para-cancer and SCLC in GSE149507. (C, D) Effects of chidamide on the expression of four HDACs in SCLC cells. Data are the mean±SD values. Unpaired two-tailed Student's *t*-test was used. *P < 0.05, **P < 0.01, ***P < 0.001. These experiments were performed three times. SCLC, small cell lung cancer; Chi, chidamide.

SCLC cell lines were treated with various concentrations of chidamide to determined the inhibitory effect of chidamide on proliferation. CCK-8 assays indicated that chidamide inhibited the growth of SCLC cells in a time- and concentration-dependent manner (**Figure 2A-C**). A tumor xenograft model was established in BALB/c-nude mice to further determine the role of chidamide in SCLC, The results showed that tumor growth was significantly suppressed in the chidamide-treated group compared to the control group. The mice were sacrificed after 14 d of treatment with chidamide and the tumor masses were photographed and measured. The tumor masses were much larger in the control group than the chidamide group (**Figure 2D**). In addition, tumor growth was significantly delayed in the chidamide group compared to the control group (**Figure 2E**). HE staining showed no apparent liver or kidney toxicity after chidamide treatment (**Figure 2F**). The IHC results indicated markedly fewer Ki-67 positive cells in the chidamide group than the control group (**Figure 2G, H**). Taken together, these findings suggested that chidamide inhibited SCLC proliferation *in vitro* and *in vivo*. In addition, RNA sequencing indicated differential enrichment in apoptotic signaling pathway genes after chidamide treatment (**Figure 2I**). qPCR and WB results confirmed an increase in the expression of the pro-apoptotic genes, Bim and Bax, and a decrease in the expression of the anti-apoptotic gene, BCL-2, after chidamide treatment (**Figure 2J**). The effect of chidamide on apoptosis was subsequently examined by flow cytometry. Chidamide significantly promoted apoptosis in SHP77 and non-SMC cells and the proportion of apoptotic cells increased with increasing drug concentration (**Figure 2K-M**).

Chidamide promotes CCL2 expression in SCLC

RNA-seq was performed on SCLC cells with or without chidamide treatment to further investigate the effects of chidamide on the SCLC TIME. Differential gene expression analysis was then performed, which identified 1,708 and 3,551 genes significantly upregulated after chidamide treatment in SHP77 and H889 cells, respectively (**Figure 3A**). The main

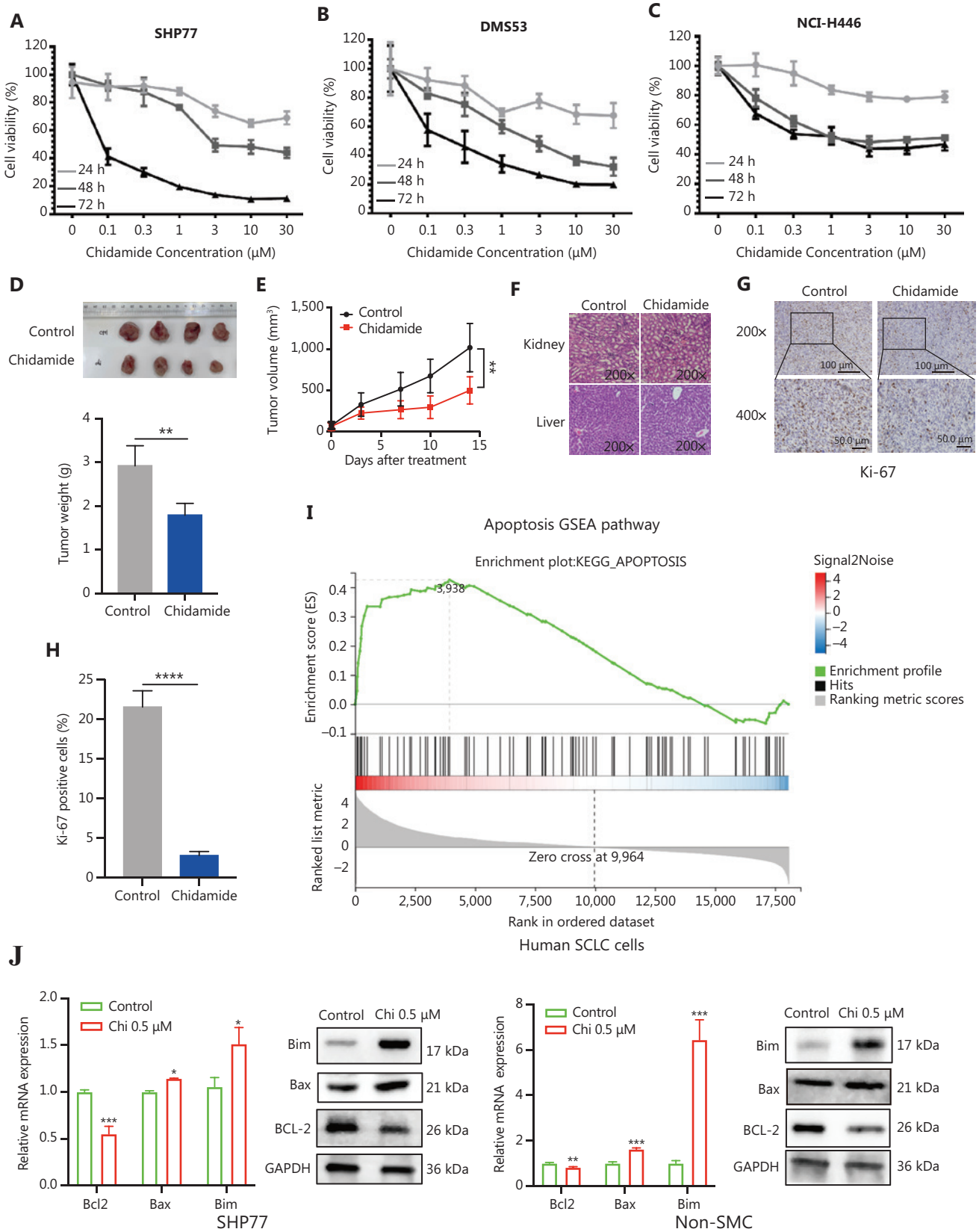

Figure 2 Continued

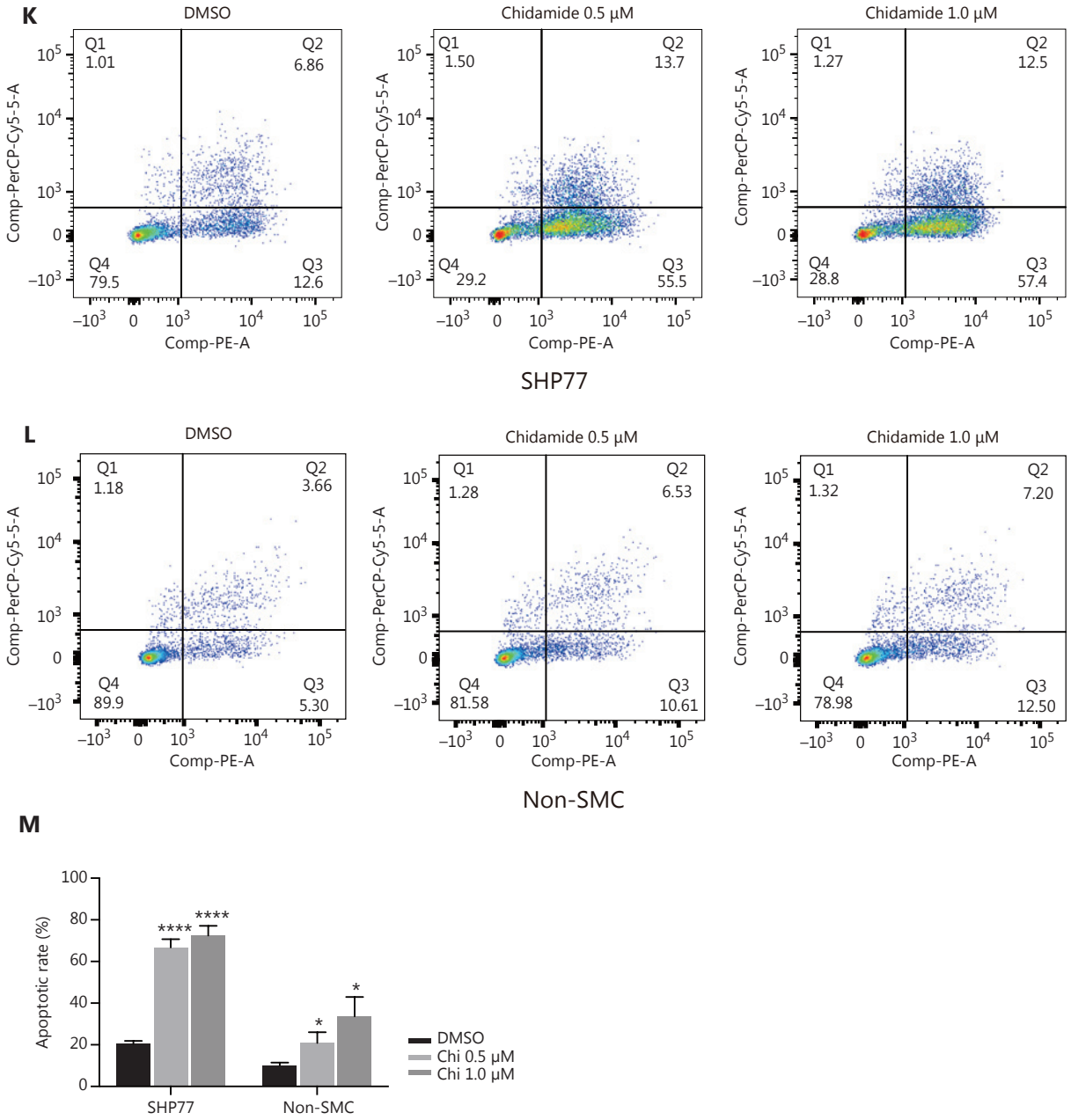

Figure 2 Chidamide inhibits malignancy proliferation in SCLC. (A-F) Effects of chidamide on the viability of various neuroendocrine SCLC cells *in vitro* (A-C), subcutaneous tumor growth, and toxicity *in vivo* (D-F). (G, H) Expression of Ki-67 in the control and chidamide groups. (I) Gene set enrichment analysis (GSEA) of apoptosis pathway transcriptomic differences in SCLC cells in the chidamide and control groups. (J) Quantification of apoptosis-associated gene expression in the chidamide and control groups according to qPCR and WB. (K-M) Flow cytometry analyses of SCLC cell apoptosis after treatment with various chidamide concentrations. Bars represent the mean±SD values. **P* < 0.05, ***P* < 0.01, ****P* < 0.001, *****P* < 0.0001. Student's *t*-test (E, H, J), one-way ANOVA (M). These experiments were performed three times.

signaling pathways of the differentially expressed genes were analyzed according to the KEGG database. The cytokine-cytokine receptor interaction pathway was a commonly enriched pathway among the three SCLC cell lines (**Figure 3B, D**). Subsequent studies focused on cytokine-cytokine receptor interaction signaling pathways, as cytokine and chemokines have been reported to be involved in regulating the TIME[29]. Human cells exhibited 25 differentially expressed genes in

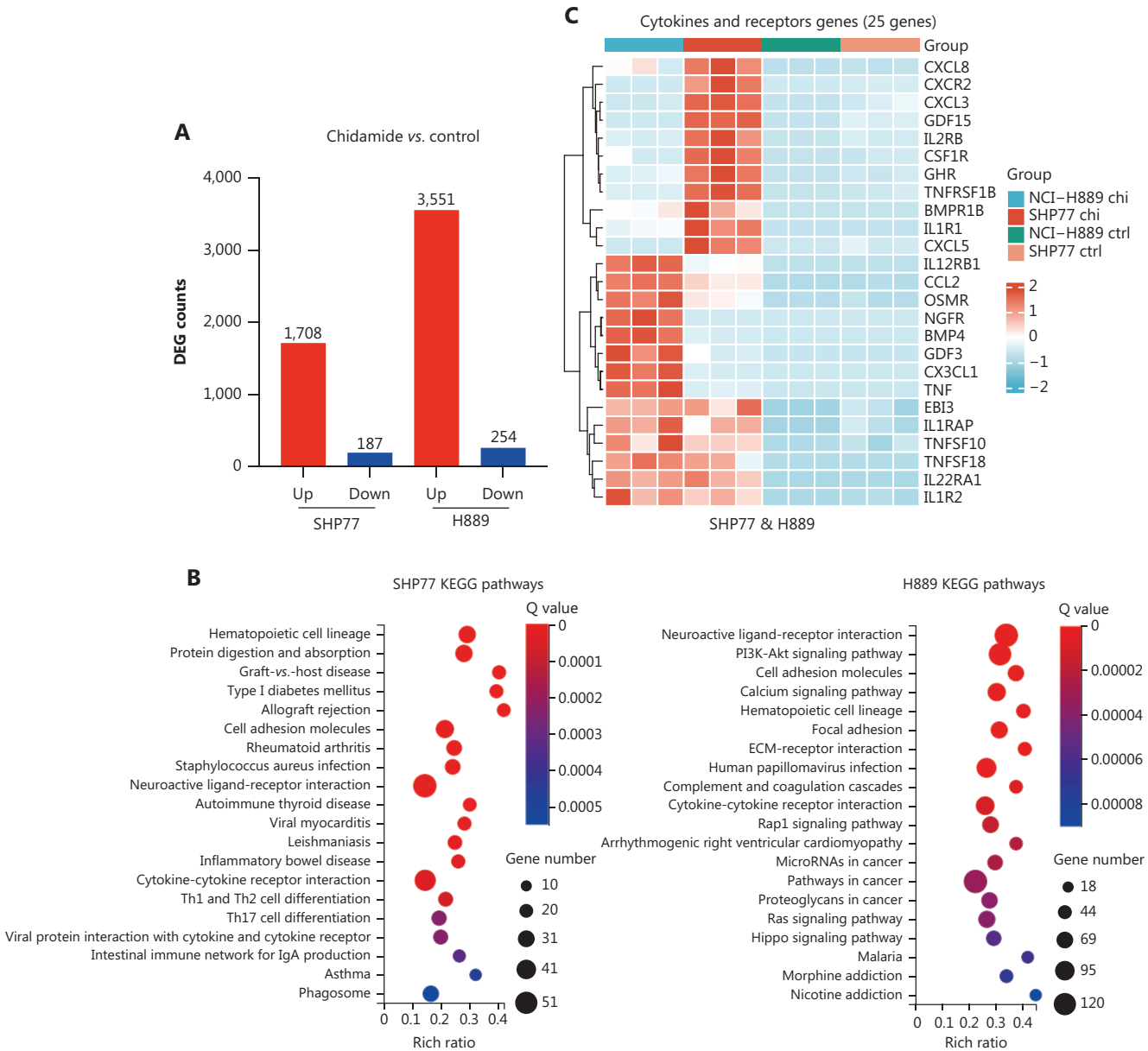

Figure 3 Continued

the cytokine-cytokine receptor interaction pathway, whereas murine cells displayed 15 differentially expressed genes (**Figure 3C, E**). By intersecting the differentially expressed cytokines, CCL2, CXCL5, and TNFRSF18 were shown to be commonly upregulated among the three SCLC cell lines after treatment with chidamide (**Figure 3F**). Subsequently, the levels of cytokine expression in the RNA-seq data were quantified and CCL2 was identified as the most significantly differentially expressed gene in SCLC cell lines (**Figure 3G, H**). The baseline expression of CCL2 in SCLC was examined according to the GEO database[30-32]. The findings revealed significantly downregulated CCL2 expression in cancer tissues compared with adjacent non-cancerous tissues (**Figure 3I**). Eighty-one patients with SCLC were subsequently stratified into high and low expression groups using x-tile software[33]. Survival curves indicated poorer prognosis among the patients with low rather than high CCL2 expression (**Figure 3J**). Moreover, the levels of CCL2 mRNA and

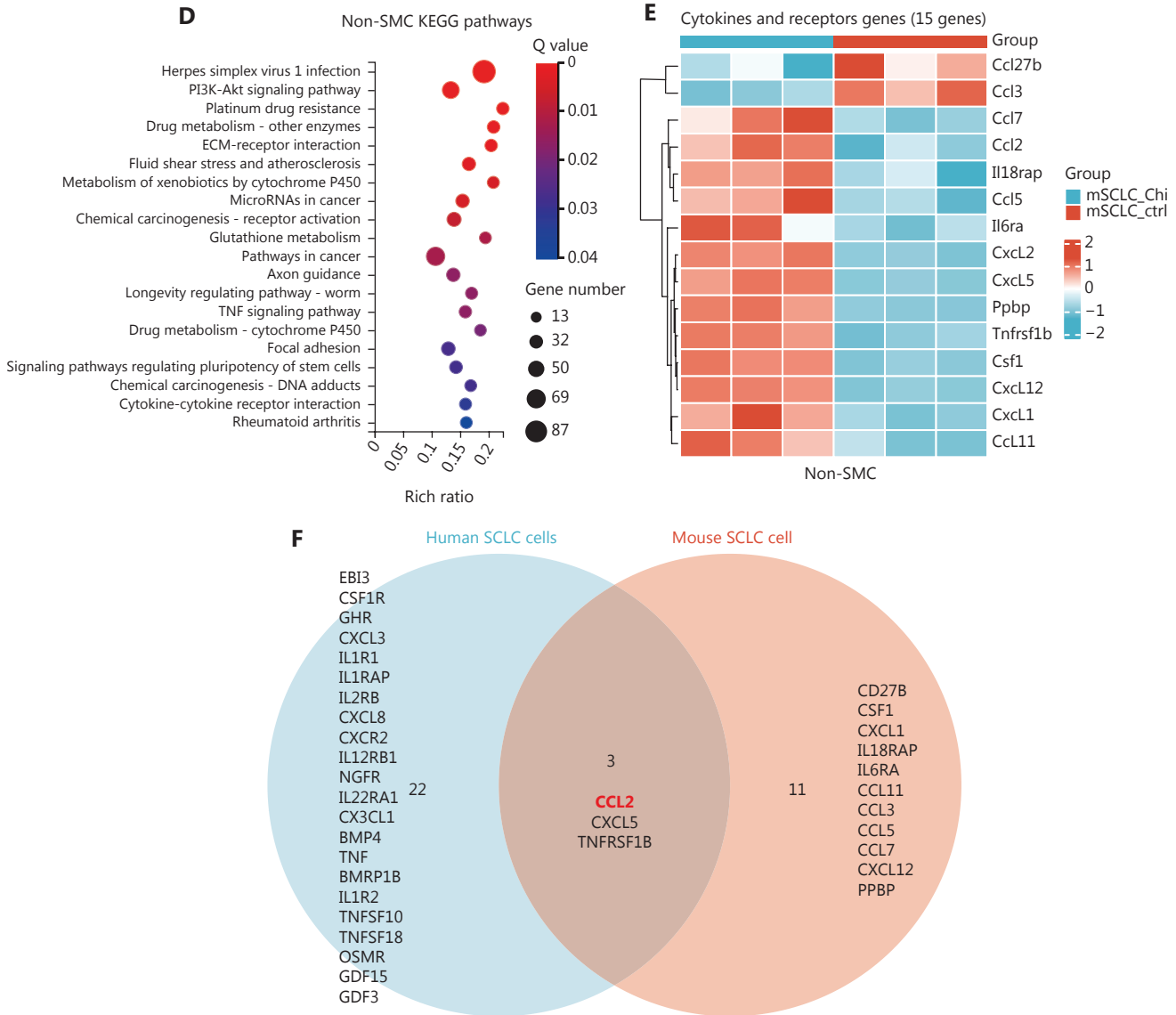

Figure 3 Continued

protein significantly increased after chidamide treatment (**Figure 3K-M**).

CCL2 promotes M1 macrophage infiltration and ameliorates the immune microenvironment

Boinformatics analysis was performed to determine the role of CCL2 in the SCLC TIME. The xCell package revealed that patients with high CCL2 expression exhibited significantly higher macrophage infiltration than patients with low CCL2 expression (**Figure 4A**) and the correlation was more pronounced between CCL2 expression and M1 macrophages (**Figure 4B**). The Cibersort package was subsequently used for further analysis. The results were consistent with the previous findings and indicated a marked increase in M1 infiltration in the SCLC TIME in patients with high CCL2 expression (**Figure 4C**). The correlation between CCL2 expression and macrophage markers was then determined to elucidate the relationship between CCL2 and macrophage infiltration in SCLC. Positive correlations were detected between CCL2 and M1 macrophage markers, including CD86 (r = 0.788, P < 0.001), CD80 (r = 0.716, P < 0.001), IL-6 (r = 0.766, P < 0.001), IL-2 (r = 0.413, P < 0.001), IL-1A (r = 0.540, P < 0.001),

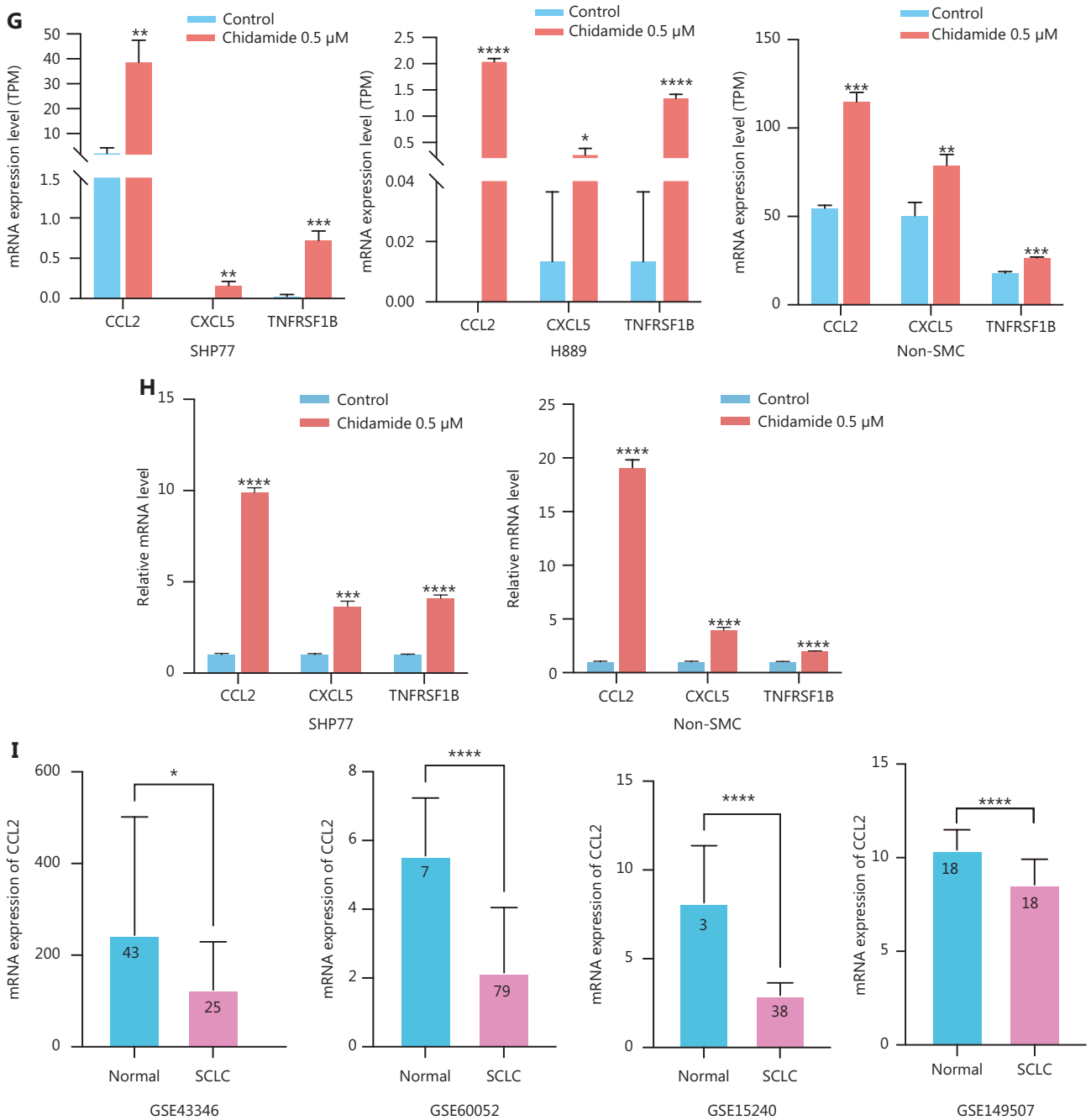

Figure 3 Continued

IL-1B ($r = 0.835$, $P < 0.001$), TLR2 ($r = 0.723$, $P < 0.001$), and TLR4 ($r = 0.477$, $P < 0.001$; **Figure 4D**). Additionally, among all M2 macrophage markers, only CD163 had a correlation with CCL2 (**Figure 4E**), Therefore, CCL2 expression in SCLC might be closely associated with infiltration of M1 macrophages in the TIME.

An initial step in immune cell function is infiltration around tumors. Therefore, Transwell assays were performed to examine the effects of cytokines secreted by SCLC cells on macrophage migration after chidamide treatment. The conditioned media obtained from SCLC cells (SHP77 and non-SMC) treated with chidamide induced macrophage

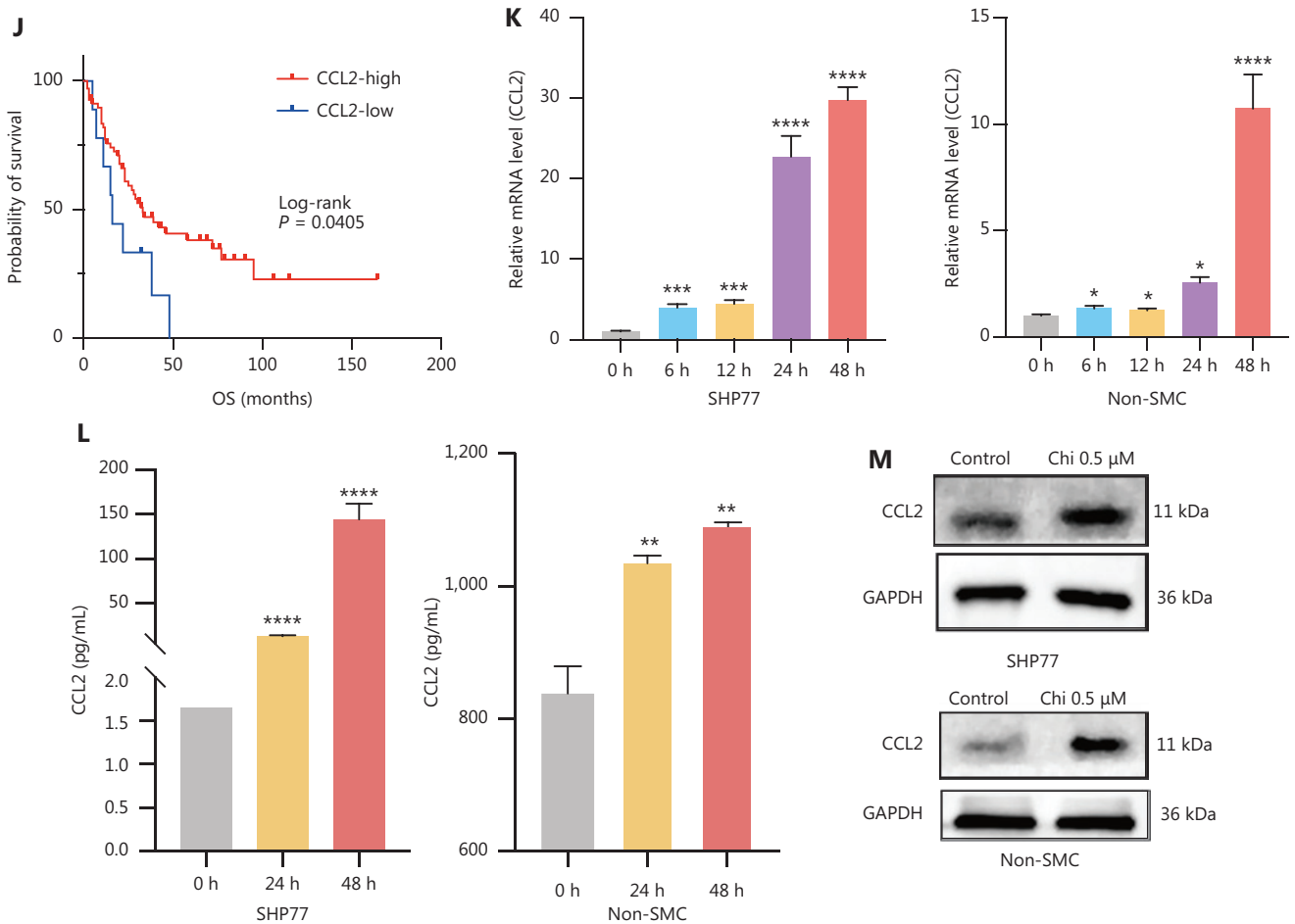

Figure 3 Chidamide promotes CCL2 expression in SCLC. (A) Differential gene expression changes in SHP77 and H889 cells before and after treatment with chidamide. KEGG signaling pathway enrichment in human (B) and murine SCLC cells (D) before and after chidamide treatment. Differential cytokine heatmap in cytokine-cytokine receptor interaction signaling pathways in human (C) and murine SCLC cells (E). (F) Venn diagram of the above-mentioned differentially expressed cytokines in the three SCLC cell lines. (G) Expression of three cytokines based on RNA sequencing. (H) Expression of three cytokines in SCLC cells verified by qPCR. (I) CCL2 expression between normal and SCLC tissues in the GSE43346(43/25), GSE60052(7/79), GSE15240(3/38), and GSE149507(18/18) datasets. (J) Survival curve of 81 SCLC patients with high or low CCL2 expression. (K-M) Changes in CCL2 expression in SCLC cells treated with chidamide for various times according to qPCR (K), ELISA (L), and WB (M). Bars represent the mean±SD values. *P < 0.05, **P < 0.01, ***P < 0.001, ****P < 0.0001. Student's t-test (G, H, I), one-way ANOVA (K, L). These experiments were performed three times (H, K, L, M).

migration more effectively than control cells (**Figure 5A, B**). Next, tumor cells were co-cultured with macrophages. qPCR indicated that chidamide significantly promoted CD86, iNOS, IL-6, and TNF-α mRNA expression in the murine co-culture system, whereas CD206, CD163, Arg1, and TGF-β1 expression was suppressed (**Figure 5C, D**). Chidamide promoted CD86 and IL-6 expression whereas inhibited the expression of CD163 and TGF-β in a co-culture system with human cells (**Figure 5E, F**). These results suggested that chidamide might exert effects on macrophage polarization. Flow cytometry was also performed to determine the effects of chidamide on macrophage polarization in the SCLC TIME. Chidamide increased the proportion of CD86-positive (CD86+) macrophages, while decreasing the proportion of CD163-positive (CD163+) cells. Additionally, the proportion of CD86+ cells significantly decreased from 9.29% to 2.3% after the addition of SHP77 tumor cells. A notable increase in CD86+ macrophages (2.3% to 7.68%)

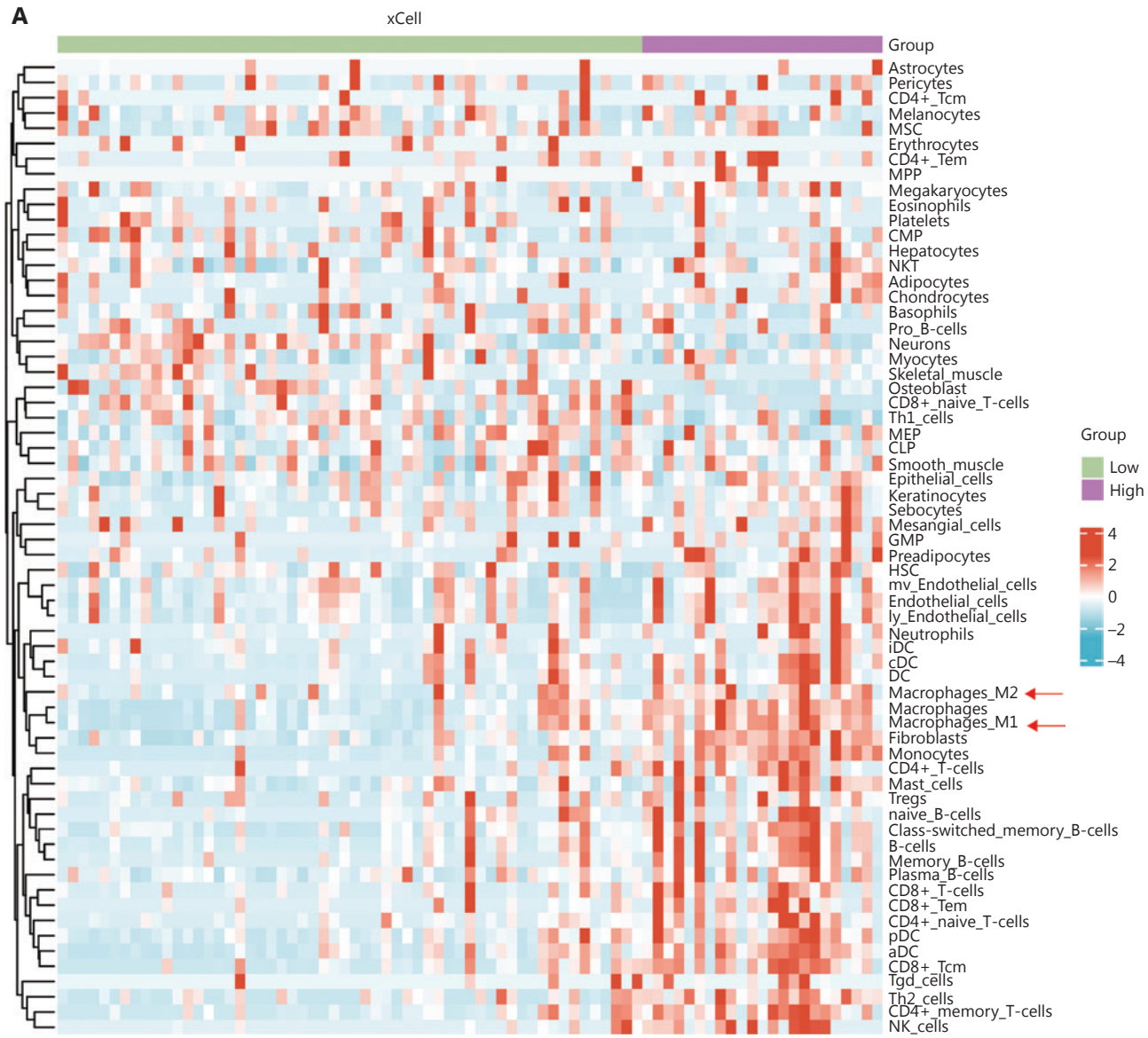

Figure 4 Continued

and a decrease in CD163+ macrophages (3.89% to 1.54%; **Figure 5G, H**) were observed after the introduction of chidamide into this co-culture system. These findings provided further support that chidamide facilitates M1 polarization of macrophages in the SCLC TIME. Flow cytometry results from mouse-derived cells demonstrated that chidamide promoted the polarization of RAW264.7 cells toward the M1 phenotype on the basis of a decrease in CD163+ cells (7.15% vs 1.73%) and an increase in CD86+ cells (43% vs 66.4%) (**Figure 5I, J**).

Chidamide promotes M1 macrophage polarization in the SCLC TIME *via* CCL2

We speculated that the chemokine, CCL2, might have a crucial role in the SCLC TIME based on RNA-seq and validation. Therefore, CCL2 neutralizing antibody was added into the co-culture system and the effect of chidamide on macrophage polarization was determined. The flow cytometry results revealed no significant change in the proportions of CD163+ and CD86+ macrophages (M0) in the tumor cells

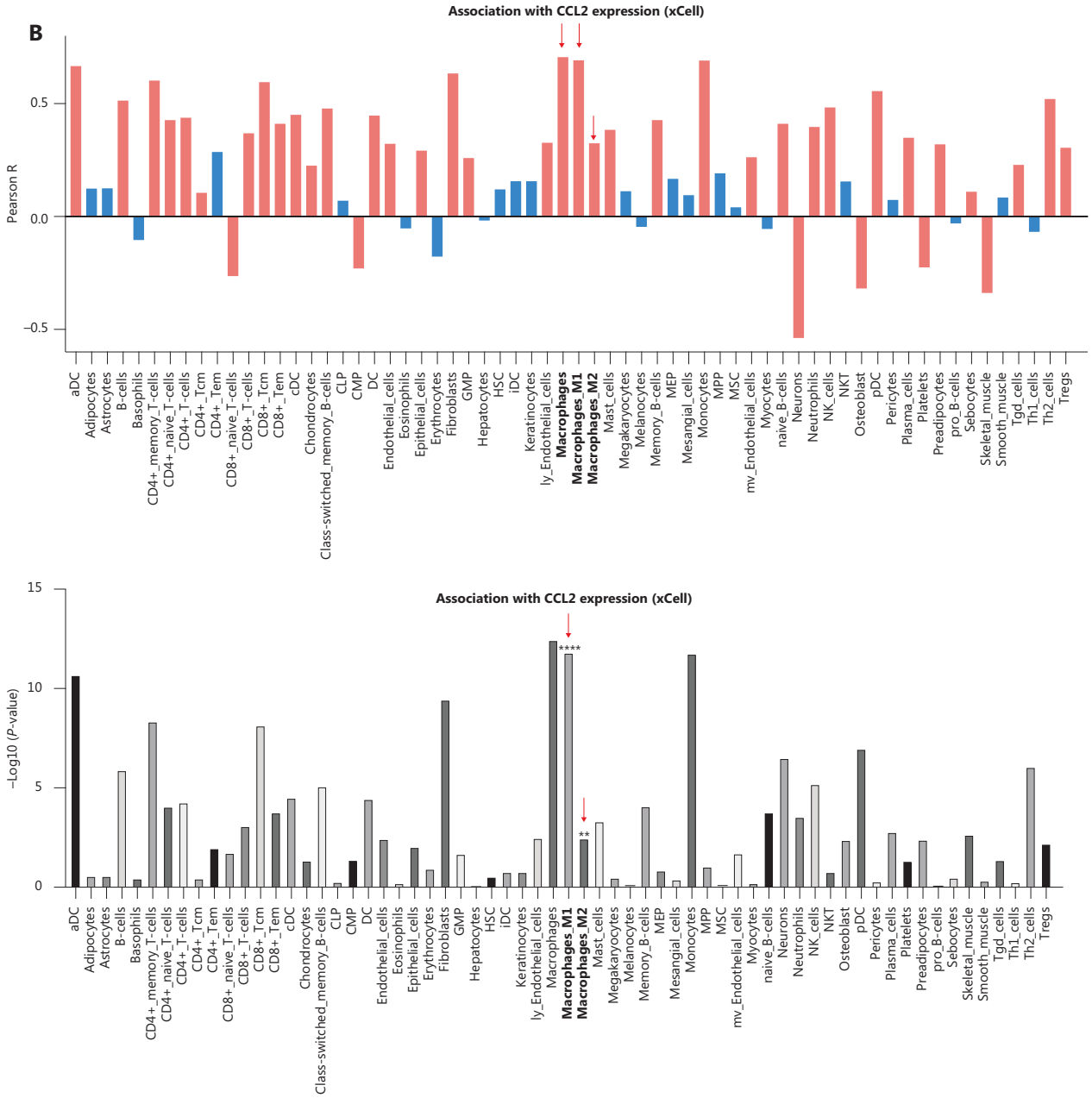

Figure 4 Continued

after addition of CCL2-neutralizing antibodies. Simultaneous treatment with chidamide and CCL2-neutralizing antibodies led to an increase in CD163+ macrophages cells compared to conditions without neutralizing antibodies (**Figure S1A**). Further validation in mouse-derived cells demonstrated that the addition of CCL2-neutralizing antibodies resulted in a increase in the proportion of CD163+ cells, whereas the proportion of CD86+ cells notably decreased (**Figure S1B**). These results confirmed that the key role of chidamide in promoting M1 macrophage infiltration is mediated by CCL2 in the SCLC immune microenvironment.

IHC of mice tumor tissues was performed to clarify the *in vivo* effects of chidamide on macrophages in the SCLC tumor microenvironment. The results revealed a significantly higher proportion of CD86+ macrophages in the chidamide group than the control group, whereas the proportion of CD163+ macrophages was relatively lower in the chidamide group (**Figure S1C-E**).

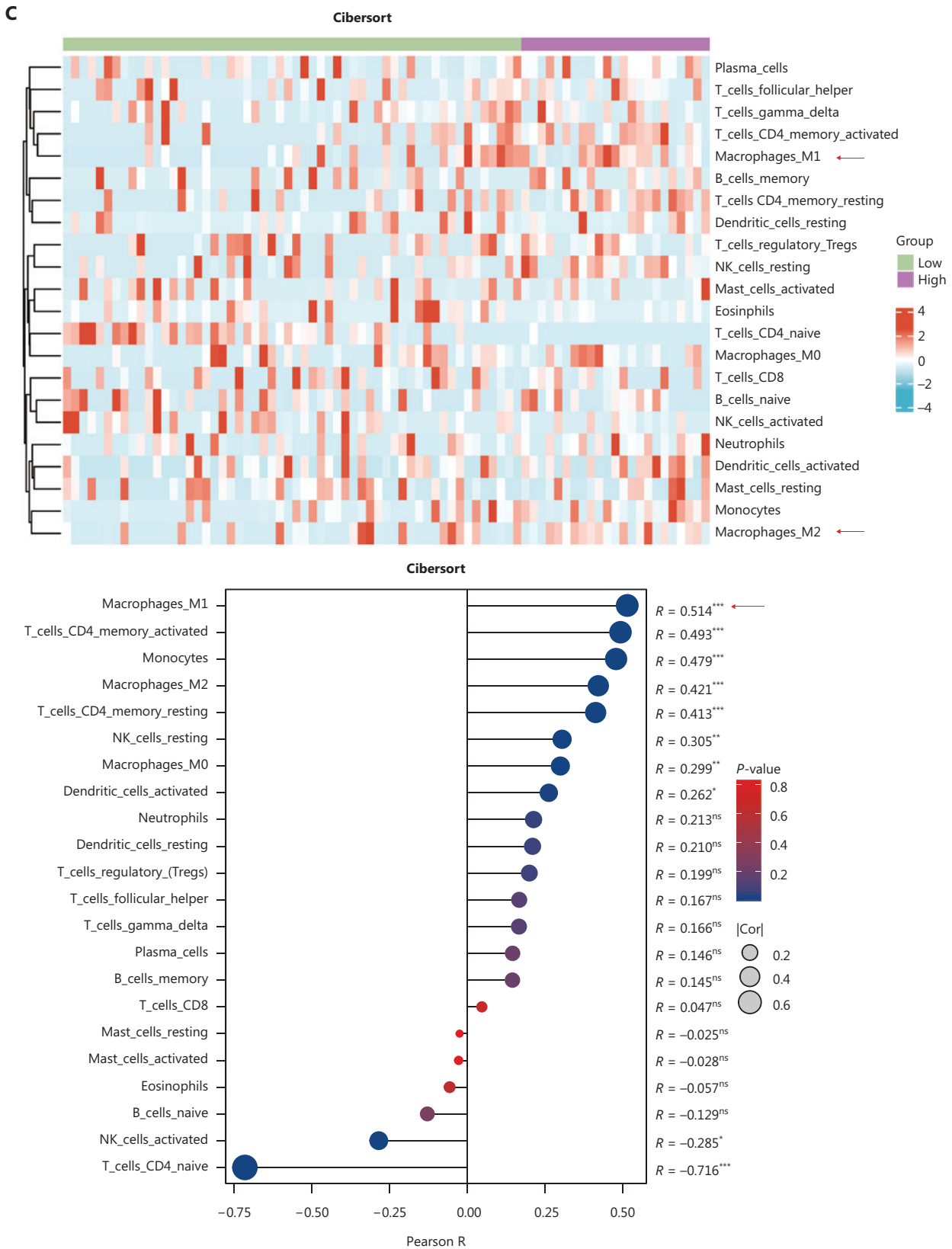

Figure 4 Continued

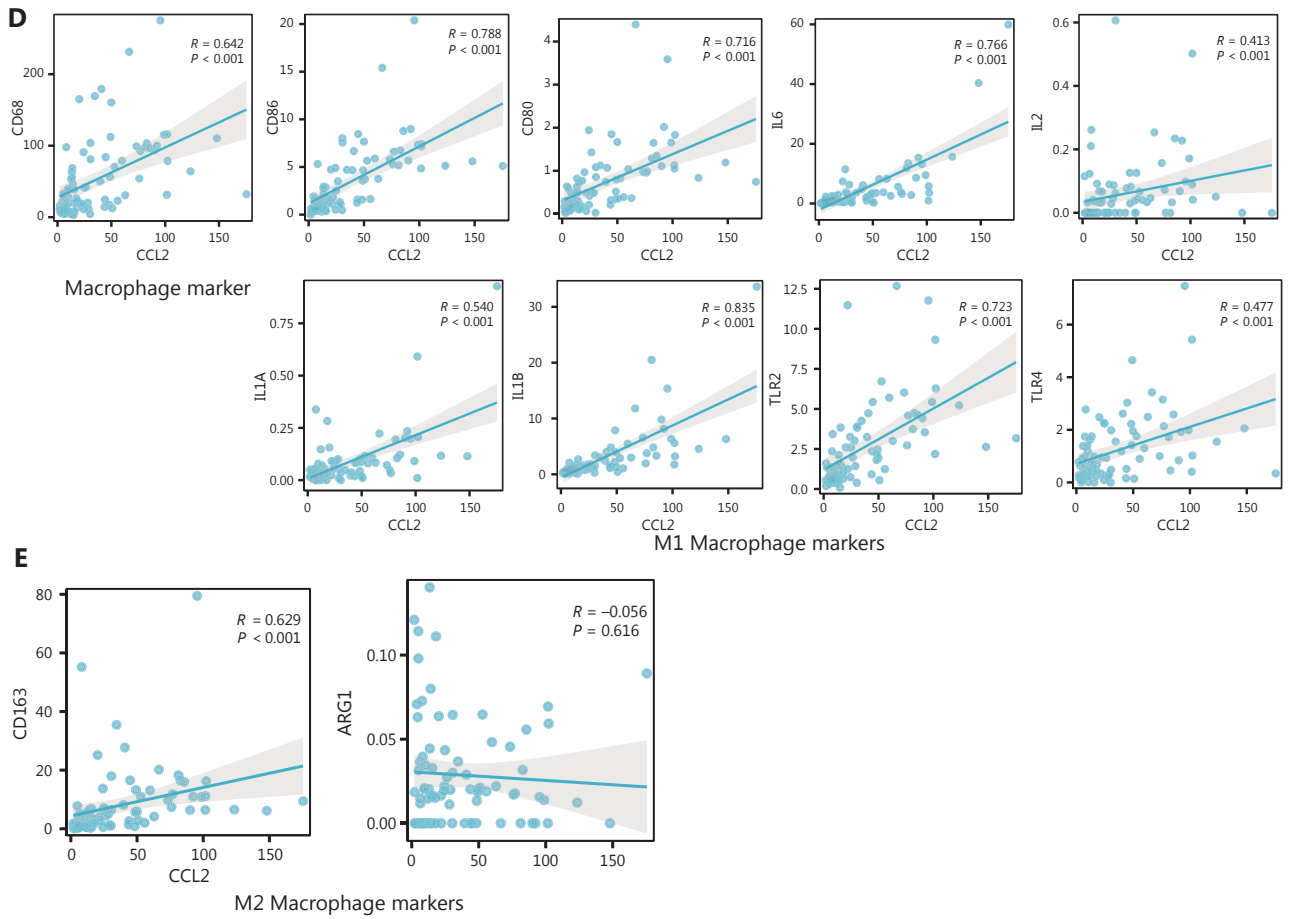

Figure 4 Relationship between CCL2 and macrophage infiltration in SCLC. (A-C) Relationship between chemokine CCL2 expression and immune cell infiltration levels in patients with SCLC analyzed with the xCell (A, B) and Cibersort packages (C). (D) Correlation between CCL2 and macrophage markers. *P < 0.05, **P < 0.01, ***P < 0.001. Pearson's rank correlation test (D).

Chidamide enhances CCL2 expression by increasing STAT4 binding to the CCL2 promoter region

To elucidate the mechanism of CCL2 regulated by chidamide, we analyzed the differential transcription factors (TFs) from RNA-seq of human SCLC cells with and without chidamide, using the criteria of $|\log_2 FC| > 2.5$ and a q-value < 0.1. TF enrichment analysis was performed with the ClusterProfiler package[34]. Numerous TFs were differentially enriched in domains after chidamide treatment, such as TEA (Transcription Enhancer Factor Domain)/ATTS (AbaA,TEC1p, TEF-1 sequence), DM(Doublesex/Mab-3) DNA-binding domain, homeobox, and STAT proteins (**Figure 6A**). The PROMO database was subsequently screened and the AnimalTFDB database predicted TFs for STAT4 by determining intersections with the above-mentioned differentially enriched TFs (**Figure 6B**). A strong positive correlation was noted between STAT4 and CCL2 in 81 RNA-seq SCLC samples (**Figure 6C**). Chidamide was subsequently verified to promote upregulation of CCL2 and STAT4 at the mRNA and protein levels with increased H3K27ac protein expression (**Figure 6D-G**). STAT4 was knocked-down with siRNA to determine the effect of STAT4 on CCL2 and the knockdown efficiency was assessed with qPCR. siRNA#275 and siRNA#2482, which had high knockdown efficiency, were selected for subsequent experiments (**Figure 6H**). CCL2 expression was clearly suppressed after knockdown of STAT4 (**Figure 6I, J**). Chidamide promoted CCL2 and STAT4 expression, whereas CCL2 expression was clearly suppressed after siRNA-STAT4 addition (**Figure 6K, L**).

The JASPAR database was initially used to predict the potential binding site between STAT4 and the promoter region of CCL2 to determine whether STAT4 modulates

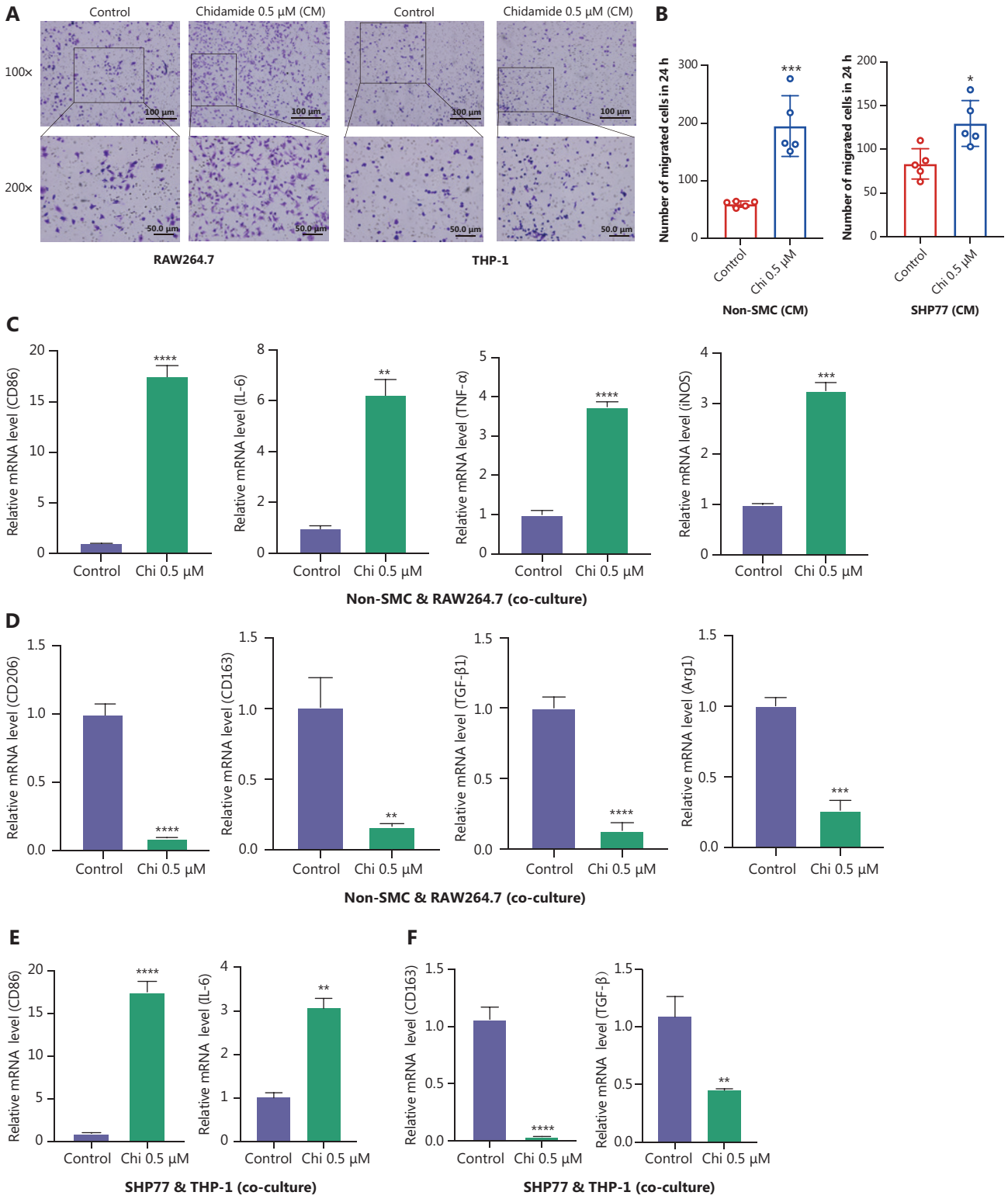

Figure 5 Continued

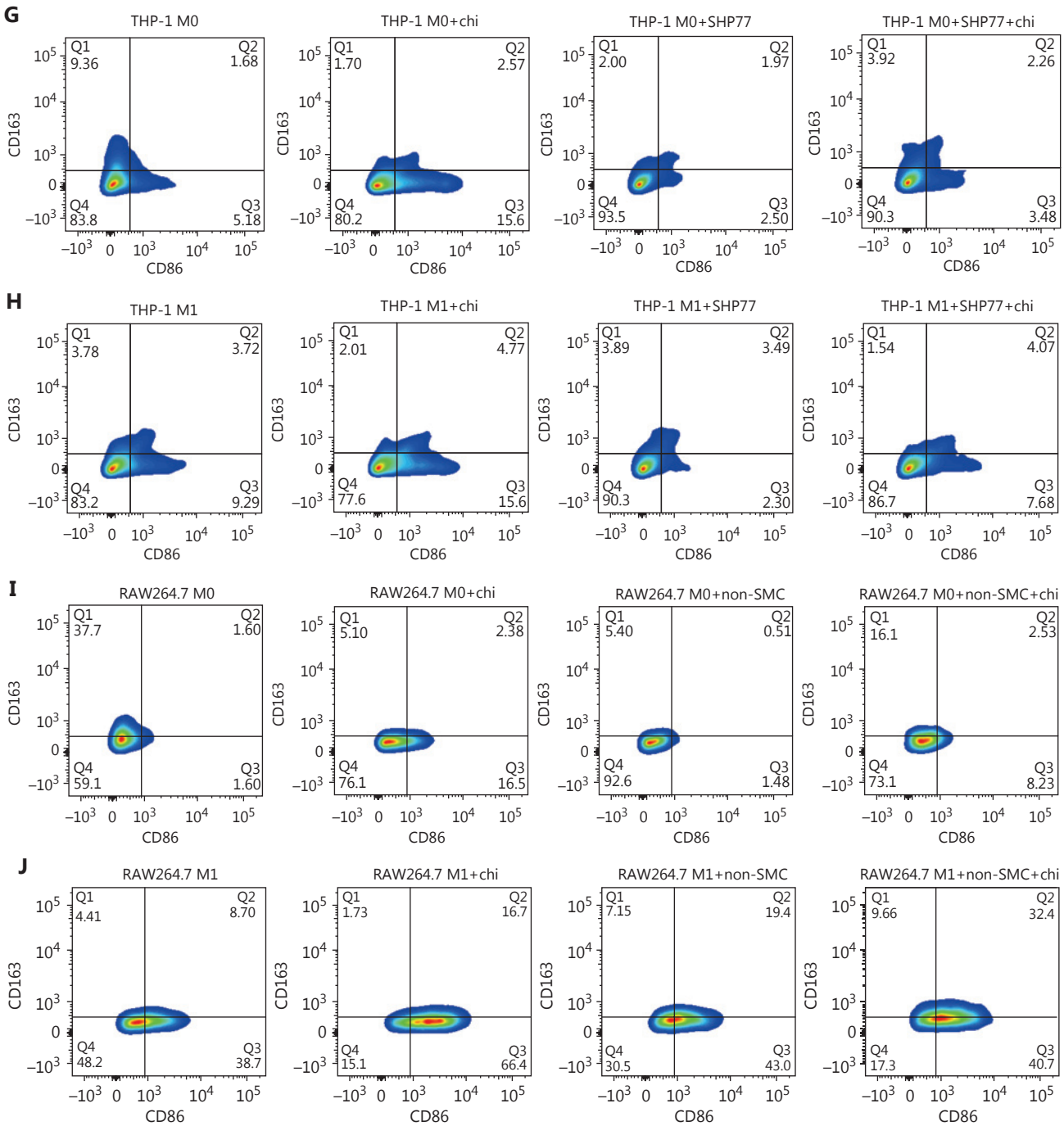

Figure 5 Chidamide augments macrophage infiltration and induces polarization to the M1 phenotype in SCLC. (A, B) Effects of conditioned medium treated with chidamide on macrophage chemotaxis detected with Transwell assays. (C-J) Effects of chidamide on macrophage polarization according to qPCR (C-F) and flow cytometry (G-J). Bars represent the mean±SD values. *P < 0.05, **P < 0.01, ***P < 0.001, ****P < 0.0001. Student's t-test (B-F). These experiments were performed three times.

CCL2 expression. Twenty-six sites were identified and the top 10 with the highest prediction scores are highlighted in **Table S4**. Ten pairs of primers for the CCL2 promoter region were subsequently designed, each approximately 500 base pairs long and spanning from 5 kb upstream to 1 kb downstream of the transcription start site (**Figure 6M**). ChIP-qPCR assays revealed a significant increase in STAT4 binding to the Up4, Up5, and Up6 primer regions of the CCL2 promoter after

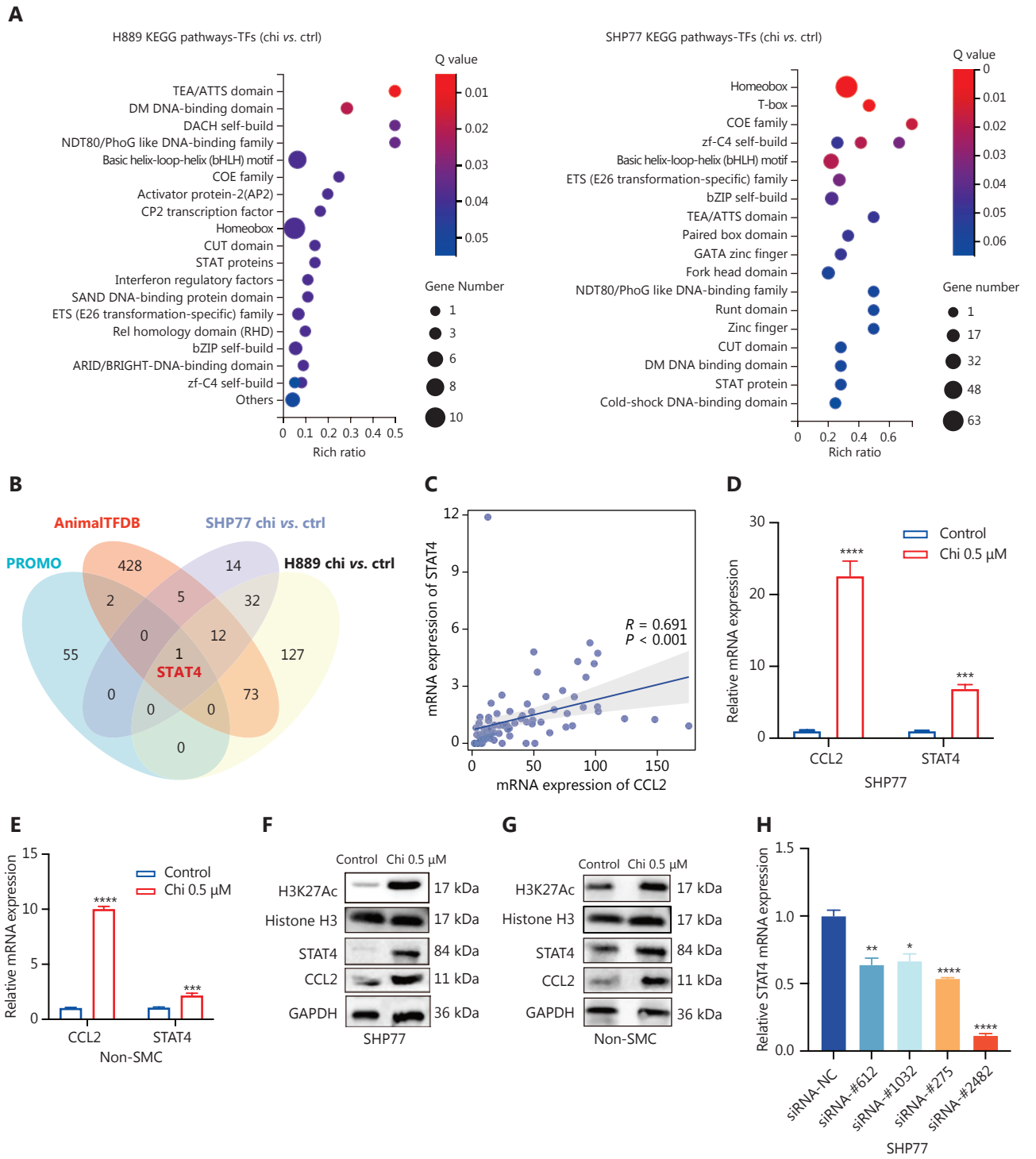

Figure 6 Continued

treatment with chidamide. Additionally, chidamide enhanced binding of H3K27ac to the Up4-Up6 primer regions upstream of the CCL2 promoter (**Figure 6N**). These findings suggested that chidamide promotes the interaction between STAT4 and CCL2 promoter, thereby activating CCL2 transcription and promoting CCL2 expression and secretion.

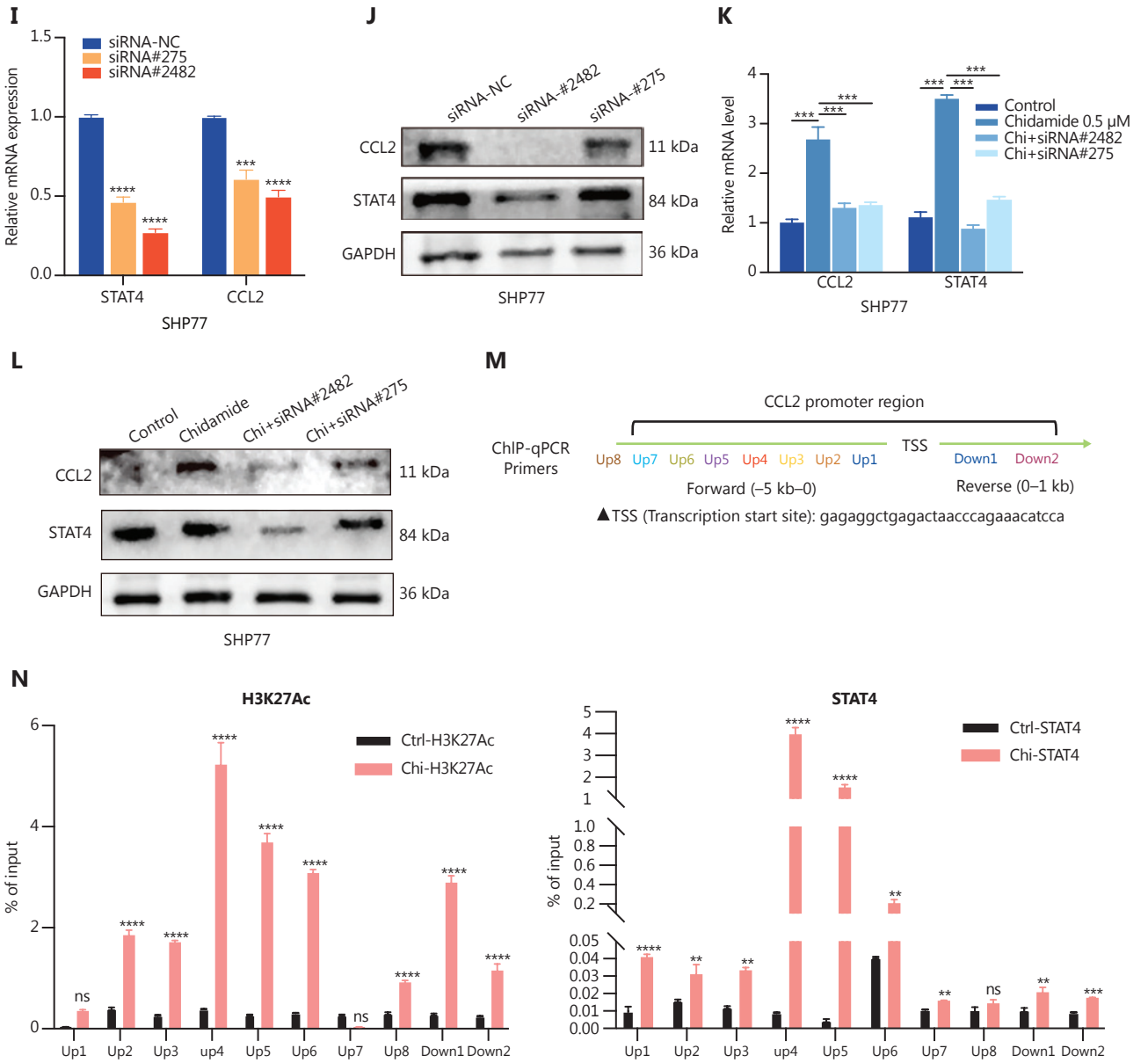

Figure 6 Chidamide promotes CCL2 expression *via* STAT4. (A) Differential transcription factor expression after chidamide treatment in SCLC cells. (B) Transcription factors identified with RNA-seq and the PROMO and AnimalTFDB databases. (C) Correlation between CCL2 and STAT4. (D-G) Chidamide influences STAT4 expression according to qPCR and WB. (H) The siRNA knockdown efficiency of STAT4 determined with qPCR. (I, J) Effects of STAT4 knockdown on CCL2 expression. (K, L) Expression of STAT4 and CCL2 across groups. (M) Schematic of ChIP-qPCR primers for the chemokine CCL2 promoter region. (N) ChIP-qPCR detection of STAT4 binding to the CCL2 promoter region. Bars represent the mean±SD values. *P < 0.05, **P < 0.01, ***P < 0.001, ****P < 0.0001. Student's t-test (D, E, H, I), one-way ANOVA (K).

Anlotinib enhances the antitumor effect of chidamide in SCLC

CCL2 has been shown to promote angiogenesis in multiple cancers[35-37]. The correlation between CCL2 and 36 angiogenesis-associated genes (AAGs) were analyzed to determine the involvement of CCL2 in angiogenesis within SCLC[38]. The results indicated a significant positive correlation between CCL2 and the expression of 27 genes, including key angiogenic factors, such as platelet-derived growth factor C (PDGFC), vascular endothelial growth factor C (VEGFC), and CD34 (**Figure S2**). RNA-seq data were next analyzed from SCLC cells

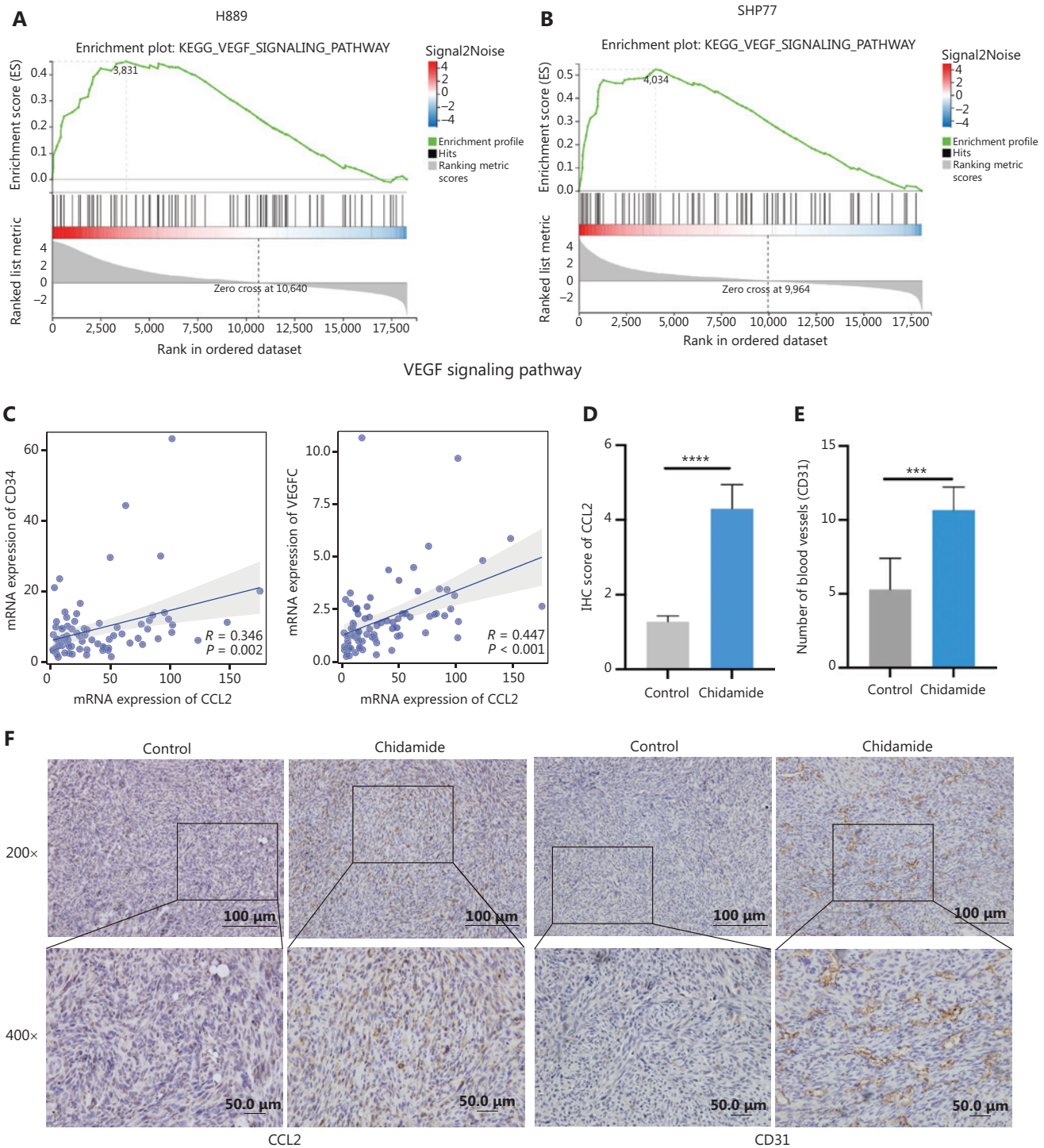

Figure 7 Continued

with or without chidamide treatment. Differentially expressed genes after chidamide treatment were significantly enriched in the VEGF signaling pathway (**Figure 7A, B**), which was closely associated with angiogenesis. A significant positive correlation was noted between CCL2 and the angiogenic genes, *CD34* and *VEGFC* (**Figure 7C**). Moreover, IHC indicated markedly higher CCL2 and CD31 protein expression in the chidamide-treated group than the control group (**Figure 7D-F**).

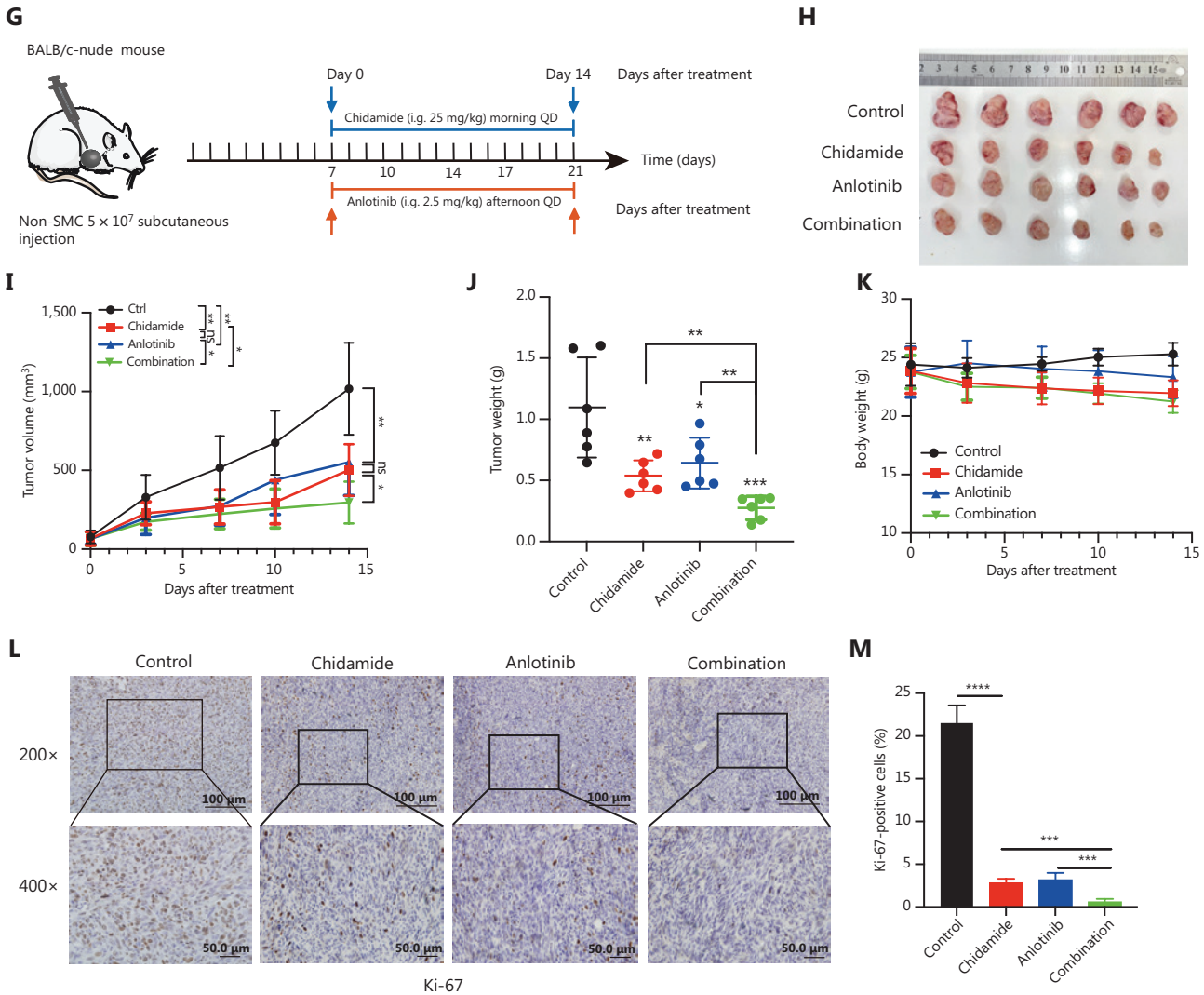

Figure 7 Anlotinib enhances the antitumor efficacy of chidamide in SCLC. (A, B) Chidamide enhances differential gene enrichment in the VEGF pathway. (C) Correlation between CCL2 and CD34 and VEGFC. (D-F) Effects of chidamide on CCL2 and CD31 protein expression *in vivo* according to IHC. (G, H) BALB/c-nude mice were implanted with 5 × 10^7 non-SMC cells and subsequently treated with chidamide alone, anlotinib alone, or a combination of both drugs. (I-K) Comparison of tumor volume growth curves, tumor weights, and mouse body weights among different groups. (L, M) Ki-67 expression in the four treatment groups. Bars represent the mean±SD values. *P < 0.05, **P < 0.01, ***P < 0.001, ****P < 0.0001. Student's t-test (D, E), one-way ANOVA (G, I), Pearson's rank correlation test (C).

Although CCL2 enhances immune surveillance by recruiting M1 macrophages, the pro-angiogenic effect may limit the efficacy of monotherapy. Therefore, the combination with anti-angiogenic drugs is a potential strategy. Previous studies have confirmed the ability of anlotinib to suppress CCL2-induced angiogenesis. Thus, the anti-tumor effects of combining anlotinib with chidamide in SCLC were further investigated[37] (**Figure 7G**). Treatment with either anlotinib or chidamide alone suppressed tumor growth compared to the control and the combined therapy impeded tumor progression more significantly (**Figure 7H-J**). Moreover, combined treatment did not lead to significant changes in body weight in tumor-bearing mice (**Figure 7K**). IHC showed that the proportion of Ki-67-positive cells in the group receiving combined treatment was notably diminished, indicating inhibition of tumor cell proliferation (**Figure 7L, M**).

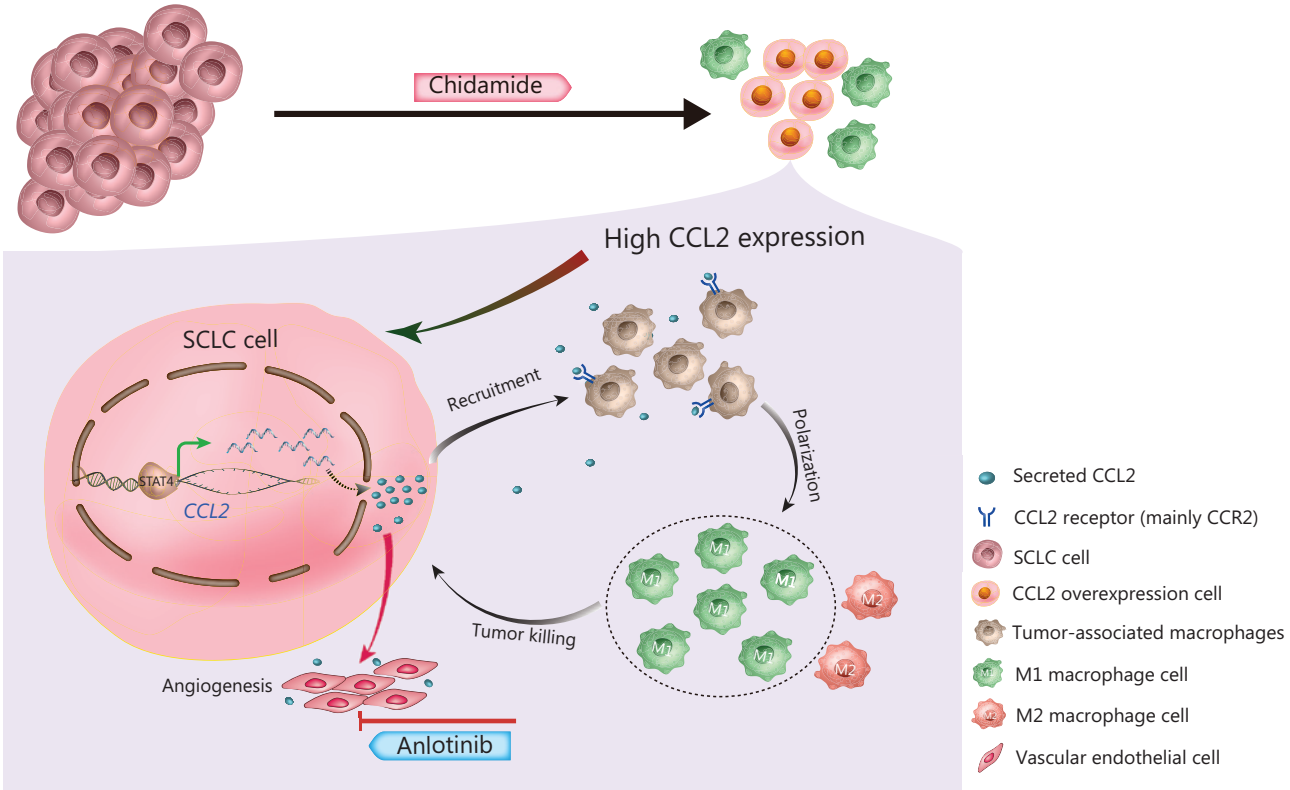

Figure 8 Schematic illustration of the mechanism underlying chidamide in SCLC. Chidamide, a first-in-class HDAC1/2/3/10 selective inhibitor, promotes CCL2 expression and secretion in SCLC cells by enhancing the transcription factor, STAT4, binding to the CCL2 promoter. Elevated CCL2 recruits macrophages mainly through the CCR2 receptor and polarizes macrophages to M1 subtypes by an unidentified mechanism in the SCLC tumor immune microenvironment, inducing anti-tumor immunity. Moreover, increased CCL2 promotes tumor angiogenesis. The combination of anlotinib and chidamide exerts a synergistic anti-tumor effect in SCLC preclinical model. CCL2, chemokine (C-C motif) ligand 2; CCR2, C-C chemokine receptor type 2; SCLC, small cell lung cancer; STAT4, signal transducer and activator of transcription 4.

Discussion

Epigenetic dysregulation has critical roles in tumorigenesis and modulation of the immune TIME[39,40]. Among various epigenetic alterations, abnormal histone modifications are a prominent mechanism underlying cancer progression. Notably, HDAC inhibitors have gained FDA approval for hematologic malignancy treatment[41] and chidamide was the first domestically developed HDAC inhibitor approved for various hematologic cancers[42,43]. In addition to the established efficacy in hematologic malignancies, chidamide has shown promising antitumor activity in solid tumors through multiple mechanisms, including suppression of drug resistance genes and enhancement of therapeutic responses through modulation of gene methylation[44-47]. In SCLC, in which epigenetic abnormalities are particularly pronounced, the therapeutic potential of HDAC inhibition is underexplored. Our analysis revealed significantly greater expression of the chidamide targets, HDAC1 and HDAC2, in SCLC than adjacent non-tumorous tissues, thus suggesting the potential involvement of them in SCLC pathogenesis. Although the expression of HDAC6 (a non-target of chidamide) has also elevated in SCLC, the functional implications require further investigation. Our findings demonstrated that chidamide exerted *in vitro* and *in vivo* anti SCLC activity through apoptosis induction and proliferation suppression.

Tumor-associated macrophages, the predominant immune population in the TIME, exhibit functional plasticity through M1/M2 polarization in response to microenvironmental cues[48,49]. M2 macrophages facilitate immune evasion and tumor progression, whereas M1 macrophages mediate antitumor immunity through T cell activation and inflammatory responses[49]. The chemokine, CCL2, which is secreted primarily by tumor cells, regulates monocyte recruitment

and tumor growth inhibition[50]. Clinical evidence has associated macrophage infiltration levels with survival outcomes in patients with SCLC[13,51]. Our investigation revealed that chidamide treatment significantly stimulates CCL2 gene expression and CCL2 protein secretion in SCLC cells and subsequently enhances macrophage infiltration into tumor sites, which is a critical prerequisite for antitumor immune responses. Mechanistic analysis demonstrated a positive correlation between CCL2 levels and M1 polarization markers. Notably, CCL2 blockade *via* neutralizing antibodies abolished chidamide-induced M1 polarization, thereby confirming CCL2 as the central mediator of this immunomodulatory process. Our findings collectively indicated that chidamide remodels the SCLC TIME through CCL2-dependent macrophage recruitment and polarization, thus shifting the balance toward antitumor M1 phenotypes.

Increased histone acetylation can activate gene transcription by facilitating TF binding to DNA. Whether histone deacetylase inhibitor chidamide might exert effects through TF activation was determined to elucidate the mechanism underlying chidamide-mediated CCL2 regulation. Integrated analysis of RNA-seq data and TF databases identified STAT4 as a candidate regulator. STAT4, a member of the signal transducer and activator of transcription family, drives IFN-γ production and promotes M1 macrophage polarization, which has pro-inflammatory phenotype and associated with impaired tissue repair and chronic inflammation[52-55]. A recent study shows that cancer patients with high STAT4 expression have significantly better prognosis than patients with low STAT4 expression after immunotherapy[56]. STAT4 expression has a strong positive correlation with CCL2 levels in SCLC models. Chidamide treatment led to significantly increased STAT4 and CCL2 expression concomitant with elevated H3K27ac binding levels at promoter regions. Functional validation through STAT4 knockdown demonstrated decreased basal CCL2 expression and attenuated chidamide-induced CCL2 upregulation. Bioinformatics analysis of the CCL2 promoter revealed multiple conserved STAT4 binding motifs. After chidamide treatment, ChIP-qPCR confirmed enhanced STAT4 occupancy at Up4-Up6 primer region and concurrent H3K27ac accumulation. These findings demonstrated that chidamide promoted STAT4-mediated transcriptional activation of CCL2 through chromatin remodeling, thus potentially driving M1 macrophage polarization in the SCLC TIME.

Differentially expressed genes were identified in angiogenesis pathways after chidamide treatment in SCLC cells using RNA-seq. Furthermore, a positive correlation was noted between CCL2 expression and various AAGs. Anlotinib, a multi-targeted therapeutic agent, has anti-tumor and angiogenesis-inhibitory effects and is a third-line therapy for SCLC. Prior research has indicated that anlotinib inhibits the angiogenic effects of CCL2 in non-small cell lung cancer[37]. Our findings revealed that anlotinib in combination with chidamide achieves a more robust anti-tumor response compared to monotherapy. This synergistic treatment addresses the angiogenesis challenge induced by CCL2, increases the anti-cancer potency of chidamide, and improves the immunosuppressive tumor microenviroment of SCLC.

One limitation of this study was that we only observed short-term effects of chidamide combined with anlotinib in animal studies and this drug combination strategy has not been tried in clinical patients. Therefore, further research is required. In the future we will gather further experimental evidence to verify the application prospects of chidamide in SCLC.

Conclusions

Our study revealed a dual role for chidamide in SCLC. One the one hand, it directly suppressed tumor growth by inhibiting proliferation and inducing apoptosis. On the other hand, it modulated the tumor microenvironment by promoting CCL2 secretion, recruiting macrophages and driving their polarization into the anti-tumor M1 phenotype. Mechanistically, chidamide regulated macrophage infiltration and polarization *via* the CCL2/STAT4 signaling axis (**Figure 8**). Our findings enhance the understanding of epigenetic therapy in SCLC and underscore the potential to target the TIME. Moreover, this work will pave the way to the development of novel combination therapies for refractory SCLC patients.

Acknowledgments

We thank Professor Hongbin Ji from the Center for Excellence in Molecular Cell Science at the Chinese Academy of Sciences for providing murine-derived SCLC cells (non-SMC). We thank International Science Editing (http://www.internationalscienceediting.com) for editing this manuscript.

Grant support

This work was supported in part by grants from National Natural Science Foundation of China (Grant Nos. 82172635, 82272686, and 82203628), the Natural Science Foundation of Tianjin (Grant Nos. 23JCZDJC00200 and 21JCYBJC01000), and the Tianjin Key Medical Discipline (Specialty) Construction Project (Grant No. TJYXZDXK-010A).

Conflict of interest statement

No potential conflicts of interest are disclosed.

Author contributions

Conceived and designed the analysis: Wenting Liu, Ting Mei, Tingting Qin, Dingzhi Huang.
Collected the data: Wenting Liu, Ting Mei, Yantao Jiang, Jingya Wang, Liuchun Wang, Zhaoting Meng, Mengjie Li.
Contributed data or analysis tools: Jiangya Wang, Tingting Qin, Dingzhi Huang.
Performed the analysis: Wenting Liu, Ting Mei.
Wrote the paper: Wenting Liu.

Data availability statement

The data generated in this study are available upon reasonable request from the corresponding author.

References

1. Meijer JJ, Leonetti A, Airò G, Tiseo M, Rolfo C, Giovannetti E, et al. Small cell lung cancer: novel treatments beyond immunotherapy. Semin Cancer Biol. 2022; 86: 376-85.
2. Kim SY, Park HS, Chiang AC. Small cell lung cancer: a review. JAMA. 2025; 333: 1906-17.
3. Marcus L, Fashoyin-Aje LA, Donoghue M, Yuan M, Rodriguez L, Gallagher PS, et al. FDA approval summary: pembrolizumab for the treatment of tumor mutational burden-high solid tumors. Clin Cancer Res. 2021; 27: 4685-9.
4. Sen T, Takahashi N, Chakraborty S, Takebe N, Nassar AH, Karim NA, et al. Emerging advances in defining the molecular and therapeutic landscape of small-cell lung cancer. Nat Rev Clin Oncol. 2024; 21: 610-27.
5. Chan JM, Quintanal-Villalonga Á, Gao VR, Xie Y, Allaj V, Chaudhary O, et al. Signatures of plasticity, metastasis, and immunosuppression in an atlas of human small cell lung cancer. Cancer Cell. 2021; 39: 1479-96.
6. Zugazagoitia J, Osma H, Baena J, Ucero AC, Paz-Ares L. Facts and hopes on cancer immunotherapy for small cell lung cancer. Clin Cancer Res. 2024; 30: 2872-83.
7. Kim HS, Lee JH, Nam SJ, Ock CY, Moon JW, Yoo CW, et al. Association of PD-L1 expression with tumor-infiltrating immune cells and mutation burden in high-grade neuroendocrine carcinoma of the lung. J Thorac Oncol. 2018; 13: 636-48.
8. Gay CM, Stewart CA, Park EM, Diao L, Groves SM, Heeke S, et al. Patterns of transcription factor programs and immune pathway activation define four major subtypes of SCLC with distinct therapeutic vulnerabilities. Cancer Cell. 2021; 39: 346-60.e7.
9. Mahadevan NR, Knelson EH, Wolff JO, Vajdi A, Saigí M, Campisi M, et al. Intrinsic immunogenicity of small cell lung carcinoma revealed by its cellular plasticity. Cancer Discov. 2021; 11: 1952-69.
10. Krushkal J, Silvers T, Reinhold WC, Sonkin D, Vural S, Connelly J, et al. Epigenome-wide DNA methylation analysis of small cell lung cancer cell lines suggests potential chemotherapy targets. Clin Epigenetics. 2020; 12: 93.
11. Qin T, Wang J, Wang J, Du Q, Wang L, Liu H, et al. Nuclear to cytoplasmic transport is a druggable dependency in HDAC7-driven small cell lung cancer. Adv Sci (Weinh). 2025; 12: e2413445.
12. Nguyen EM, Taniguchi H, Chan JM, Zhan YA, Chen X, Qiu J, et al. Targeting lysine-specific demethylase 1 rescues major histocompatibility complex class I antigen presentation and overcomes programmed death-ligand 1 blockade resistance in SCLC. J Thorac Oncol. 2022; 17: 1014-31.
13. Zheng Y, Wang Z, Wei S, Liu Z, Chen G. Epigenetic silencing of chemokine CCL2 represses macrophage infiltration to potentiate tumor development in small cell lung cancer. Cancer Lett. 2021; 499: 148-63.
14. Zhao PY, Sun XD, Li H, Tian L, Lu YH, Cheng Y. [The effect of c-Myc on regulating the immune-related ligands in Y subtype small cell lung cancer through histone deacetylase 1]. Zhonghua Zhong Liu Za Zhi. 2024; 46: 1009-18.
15. Maggs L, Sadagopan A, Moghaddam AS, Ferrone S. HLA class I antigen processing machinery defects in antitumor immunity and immunotherapy. Trends Cancer. 2021; 7: 1089-101.
16. Henning AN, Roychoudhuri R, Restifo NP. Epigenetic control of $CD8^+$ T cell differentiation. Nat Rev Immunol. 2018; 18: 340-56.
17. Shang X, Cheng B, Zhang C, Zhao C, Wang R, Zhang X, et al. The LDH-H3K18La-Nur77 axis potentiates immune escape in small cell lung cancer. Adv Sci (Weinh). 2025: e13608.
18. Mei M, Chen L, Godfrey J, Song J, Egelston C, Puverel S, et al. Pembrolizumab plus vorinostat induces responses in patients with Hodgkin lymphoma refractory to prior PD-1 blockade. Blood. 2023; 142: 1359-70.
19. Manasanch EE, Shah JJ, Lee HC, Weber DM, Thomas SK, Amini B, et al. Phase I/Ib study of carfilzomib and panobinostat with or without dexamethasone in patients with relapsed/refractory multiple myeloma. Haematologica. 2020; 105: e242-5.

20. Barone S, Bello I, Guadagni A, Cerchia C, Filocamo G, Cassese E, et al. Challenging triple negative breast cancer through HDAC6 selective inhibition: novel cap-group identification, structure-activity relationships, computational and biological studies. Eur J Med Chem. 2025; 292: 117634.
21. Jiang Y, Zhang J, Yu J, Luo W, Du Q, Liu W, et al. HDAC6 facilitates LUAD progression by inducing EMT and enhancing macrophage polarization towards the M2 phenotype. NPJ Precis Oncol. 2025; 9: 150.
22. Rai S, Kim WS, Ando K, Choi I, Izutsu K, Tsukamoto N, et al. Oral HDAC inhibitor tucidinostat in patients with relapsed or refractory peripheral T-cell lymphoma: phase IIb results. Haematologica. 2023; 108: 811-21.
23. Jiang Z, Li W, Hu X, Zhang Q, Sun T, Cui S, et al. Tucidinostat plus exemestane for postmenopausal patients with advanced, hormone receptor-positive breast cancer (ACE): a randomised, double-blind, placebo-controlled, phase 3 trial. Lancet Oncol. 2019; 20: 806-15.
24. He X, Li Y, Li J, Li Y, Chen S, Yan X, et al. HDAC2-mediated METTL3 delactylation promotes DNA damage repair and chemotherapy resistance in triple-negative breast cancer. Adv Sci (Weinh). 2025; 12: e2413121.
25. Jin Y, Zhao Q, Zhu W, Feng Y, Xiao T, Zhang P, et al. Identification of TAZ as the essential molecular switch in orchestrating SCLC phenotypic transition and metastasis. Natl Sci Rev. 2022; 9: nwab232.
26. Liu W, Jiang K, Wang J, Mei T, Zhao M, Huang D. Upregulation of GNPNAT1 predicts poor prognosis and correlates with immune infiltration in lung adenocarcinoma. Front Mol Biosci. 2021; 8: 605754.
27. George J, Lim JS, Jang SJ, Cun Y, Ozretić L, Kong G, et al. Comprehensive genomic profiles of small cell lung cancer. Nature. 2015; 524: 47-53.
28. Cai L, Liu H, Huang F, Fujimoto J, Girard L, Chen J, et al. Cell-autonomous immune gene expression is repressed in pulmonary neuroendocrine cells and small cell lung cancer. Commun Biol. 2021; 4: 314.
29. Zhou C, Weng J, Liu C, Liu S, Hu Z, Xie X, et al. Disruption of SLFN11 deficiency-induced CCL2 signaling and macrophage M2 polarization potentiates anti-PD-1 therapy efficacy in hepatocellular carcinoma. Gastroenterology. 2023; 164: 1261-78.
30. Jiang L, Huang J, Higgs BW, Hu Z, Xiao Z, Yao X, et al. Genomic landscape survey identifies SRSF1 as a key oncodriver in small cell lung cancer. PLoS Genet. 2016; 12: e1005895.
31. Sato T, Kaneda A, Tsuji S, Isagawa T, Yamamoto S, Fujita T, et al. PRC2 overexpression and PRC2-target gene repression relating to poorer prognosis in small cell lung cancer. Sci Rep. 2013; 3: 1911.
32. Daniel VC, Marchionni L, Hierman JS, Rhodes JT, Devereux WL, Rudin CM, et al. A primary xenograft model of small-cell lung cancer reveals irreversible changes in gene expression imposed by culture in vitro. Cancer Res. 2009; 69: 3364-73.
33. Camp RL, Dolled-Filhart M, Rimm DL. X-tile: a new bio-informatics tool for biomarker assessment and outcome-based cut-point optimization. Clin Cancer Res. 2004; 10: 7252-9.
34. Wu T, Hu E, Xu S, Chen M, Guo P, Dai Z, et al. clusterProfiler 4.0: a universal enrichment tool for interpreting omics data. Innovation (Camb). 2021; 2: 100141.
35. Feng H, Liu K, Shen X, Liang J, Wang C, Qiu W, et al. Targeting tumor cell-derived CCL2 as a strategy to overcome Bevacizumab resistance in ETV5$^+$ colorectal cancer. Cell Death Dis. 2020; 11: 916.
36. Möckel D, Bartneck M, Niemietz P, Wagner M, Ehling J, Rama E, et al. CCL2 chemokine inhibition primes the tumor vasculature for improved nanomedicine delivery and efficacy. J Control Release. 2024; 365: 358-68.
37. Lu J, Zhong H, Chu T, Zhang X, Li R, Sun J, et al. Role of anlotinib-induced CCL2 decrease in anti-angiogenesis and response prediction for nonsmall cell lung cancer therapy. Eur Respir J. 2019; 53: 1801562.
38. Qing X, Xu W, Liu S, Chen Z, Ye C, Zhang Y. Molecular characteristics, clinical significance, and cancer immune interactions of angiogenesis-associated genes in gastric cancer. Front Immunol. 2022; 13: 843077.
39. Ramazi S, Dadzadi M, Sahafnejad Z, Allahverdi A. Epigenetic regulation in lung cancer. MedComm (2020). 2023; 4: e401.
40. Topper MJ, Vaz M, Marrone KA, Brahmer JR, Baylin SB. The emerging role of epigenetic therapeutics in immuno-oncology. Nat Rev Clin Oncol. 2020; 17: 75-90.
41. Shi Y, Jia B, Xu W, Li W, Liu T, Liu P, et al. Chidamide in relapsed or refractory peripheral T cell lymphoma: a multicenter real-world study in China. J Hematol Oncol. 2017; 10: 69.
42. Gu S, Hou Y, Dovat K, Dovat S, Song C, Ge Z. Synergistic effect of HDAC inhibitor Chidamide with Cladribine on cell cycle arrest and apoptosis by targeting HDAC2/c-Myc/RCC1 axis in acute myeloid leukemia. Exp Hematol Oncol. 2023; 12: 23.
43. Guan XW, Wang HQ, Ban WW, Chang Z, Chen HZ, Jia L, et al. Novel HDAC inhibitor Chidamide synergizes with Rituximab to inhibit diffuse large B-cell lymphoma tumour growth by upregulating CD20. Cell Death Dis. 2020; 11: 20.
44. Que Y, Zhang XL, Liu ZX, Zhao JJ, Pan QZ, Wen XZ, et al. Frequent amplification of HDAC genes and efficacy of HDAC inhibitor chidamide and PD-1 blockade combination in soft tissue sarcoma. J Immunother Cancer. 2021; 9: e001696.
45. Ding N, You A, Tian W, Gu L, Deng D. Chidamide increases the sensitivity of non-small cell lung cancer to crizotinib by decreasing *c-MET* mRNA methylation. Int J Biol Sci. 2020; 16: 2595-611.
46. Zhou J, Wu X, Zhang H, Wang X, Yuan Y, Zhang S, et al. Clinical outcomes of tucidinostat-based therapy after prior CDK4/6 inhibitor progression in hormone receptor-positive heavily pretreated metastatic breast cancer. Breast. 2022; 66: 255-61.
47. Shao J, Ye Z, Shen Z, Liu N, Zhang L, Tachibana M, et al. Chidamide improves gefitinib treatment outcomes in NSCLC by attenuating recruitment and immunosuppressive function of myeloid-derived suppressor cells. Biomed Pharmacother. 2024; 173: 116306.
48. Cassetta L, Fragkogianni S, Sims AH, Swierczak A, Forrester LM, Zhang H, et al. Human tumor-associated macrophage and

monocyte transcriptional landscapes reveal cancer-specific reprogramming, biomarkers, and therapeutic targets. Cancer Cell. 2019; 35: 588-602.e10.
49. Boutilier AJ, Elsawa SF. Macrophage polarization states in the tumor microenvironment. Int J Mol Sci. 2021; 22: 6995.
50. Matsushima K, Larsen CG, DuBois GC, Oppenheim JJ. Purification and characterization of a novel monocyte chemotactic and activating factor produced by a human myelomonocytic cell line. J Exp Med. 1989; 169: 1485-90.
51. Klein S, Schulte A, Arolt C, Tolkach Y, Reinhardt HC, Buettner R, et al. Intratumoral abundance of M2-macrophages is associated with unfavorable prognosis and markers of T-cell exhaustion in small cell lung cancer patients. Mod Pathol. 2023; 36: 100272.
52. Ploeger DT, Hosper NA, Schipper M, Koerts JA, de Rond S, Bank RA. Cell plasticity in wound healing: paracrine factors of M1/M2 polarized macrophages influence the phenotypical state of dermal fibroblasts. Cell Commun Signal. 2013; 11: 29.
53. Cunnion KM, Krishna NK, Pallera HK, Pineros-Fernandez A, Rivera MG, Hair PS, et al. Complement activation and STAT4 expression are associated with early inflammation in diabetic wounds. PLoS One. 2017; 12: e0170500.
54. Dobrian AD, Galkina EV, Ma Q, Hatcher M, Aye SM, Butcher MJ, et al. STAT4 deficiency reduces obesity-induced insulin resistance and adipose tissue inflammation. Diabetes. 2013; 62: 4109-21.
55. Dobrian AD, Hatcher MA, Brotman JJ, Galkina EV, Taghavie-Moghadam P, Pei H, et al. STAT4 contributes to adipose tissue inflammation and atherosclerosis. J Endocrinol. 2015; 227: 13-24.
56. Ding X, Zhang L, Fan M, Li L. TME-NET: an interpretable deep neural network for predicting pan-cancer immune checkpoint inhibitor responses. Brief Bioinform. 2024; 25: bbae410.

Cite this article as: Liu W, Mei T, Jiang Y, Wang J, Li M, Wang L, et al. Chidamide suppresses macrophage-mediated immune evasion and tumor progression in small cell lung cancer by targeting the STAT4/CCL2 signaling pathway. Cancer Biol Med. 2025; 22: 1578-1604. doi: 10.20892/j.issn.2095-3941.2024.0241